

# The evolution of carbon oxidation state during secondary organic aerosol formation from individual and mixed organic precursors

Yunqi Shao<sup>1</sup>, Aristeidis Voliotis<sup>1,2</sup>, Mao Du<sup>1,6</sup>, Yu Wang<sup>1,5</sup>, [Thomas J. Bannan<sup>1</sup>](#), Jacqueline Hamilton<sup>3</sup>, M. Rami Alfarra<sup>1,2,4</sup>, Gordon McFiggans<sup>1</sup>

<sup>1</sup>School of Earth and Environmental Science, University of Manchester, Manchester, M13, 9PL, UK

<sup>2</sup>National Centre for Atmospheric Science (NCAS), University of Manchester, Manchester, M13 9PL, UK

<sup>3</sup>Wolfson Atmospheric Chemistry Laboratories, Department of Chemistry, University of York, York, YO105DD, UK

<sup>4</sup>Now at Qatar Environment and Energy Research Institute, Hamad Bin Khalifa University, Doha, Qatar

<sup>5</sup>now at School of Geosciences, University of Edinburgh, Edinburgh, EH9 3FF, UK

<sup>6</sup>now at School of Geography Earth and Environment Sciences, University of Birmingham, Birmingham B15 2TT, UK

Correspondence to: Yunqi.Shao (Yunqi.Shao@Manchester.ac.uk)

## Abstract

This study reports the average carbon oxidation state ( $\overline{OSc}$ ) of secondary organic aerosol (SOA) particles formed from the photo-oxidation of *o*-cresol,  $\alpha$ -pinene, isoprene and their mixtures, representative anthropogenic and biogenic precursors, in the Manchester Aerosol Chamber. Three independent mass spectrometric techniques, including two online instruments, high resolution time-of-flight Aerodyne Aerosol Mass Spectrometers (HR-ToF-AMS) and Filter Inlet for Gases and AEROSols coupled to an Iodide high-resolution time of flight chemical ionisation mass spectrometer (FIGAERO-CIMS), and one offline technique, ultra-high-performance liquid chromatography-high resolution mass spectrometry (UHPLC-HRMS), were employed to characterise chemical composition of SOA molar atomic ratios (e.g. O/C, H/C and N/C) and derive leading to estimation of the SOA particle  $\overline{OSc}$  coverage carbon oxidation state in mixtures of  $\alpha$ -pinene/isoprene, *o*-cresol/isoprene,  $\alpha$ -pinene/*o*-cresol and  $\alpha$ -pinene/*o*-cresol/isoprene system. This paper firstly reports the detailed analysis of particle average  $\overline{OSc}$  carbon oxidation state during SOA formation in mixed anthropogenic and biogenic systems using two online and one offline mass spectrometry techniques simultaneously.

Across single precursor experiments,  $\overline{OSc}$  generally declined with increasing SOA mass, suggesting with a shift from highly oxygenated, low-volatility products at early stages toward more semi-volatile, less oxidised compounds at higher particle mass loading. at various initial concentrations were used as a reference. This behaviour was robust across different initial precursor concentrations, implying that SOA growth is dominated by partitioning dynamics rather than initial precursors' reactivity.

Moreover, comparisons across analytical techniques demonstrate systematic differences, with FIGAERO-CIMS consistently reported higher  $\overline{OSc}$ , UHPLC-HRMS (negative mode) aligned

more closely with FIGAERO-CIMS, while HR-ToF-AMS underestimated  $\overline{OSc}$  due to its inability to resolve nitrogen containing species.

Furthermore, correcting for the oxidation state of nitrogen ( $\overline{OS_N}$ ) significantly reduced  $\overline{OSc}$  estimates in *o*-Cresol experiments, likely reflecting the strong influence of CHON compound.

Mixture precursor experiments reveals the isoprene suppressed the formation of highly oxygenated  $\alpha$ -pinene products through OH scavenging and RO<sub>2</sub> competition, lowering  $\overline{OSc}$  in mixed systems. In contrast,  $\alpha$ -pinene/*o*-Cresol mixtures showed elevated  $\overline{OSc}$ , likely contributed by the cross interaction between precursor's driven RO<sub>2</sub> forming multifunctional accretion products. The ternary mixture evolved to intermediate  $\overline{OSc}$  values between the single precursor experiment, which could imply a balance between OH scavenging, RO<sub>2</sub> competition, and cross interaction reaction.

The oxidation state of nitrogen ( $\overline{OS_N}$ ) for CHON compounds was shown to non-negligibly influence the average  $\overline{OSc}$  in individual precursor  $\alpha$ -pinene and *o*-cresol experiments in FIGAERO-CIMS and UHPLC-HRMS measurements. By definition, the average  $\overline{OSc}$  accounting for  $\overline{OS_N}$ , is lower than when the  $\overline{OS_N}$  is not considered. SOA particle average oxidation state excluding consideration of  $\overline{OS_N}$  obtained by the three techniques showed substantial discrepancies. That obtained from FIGAERO-CIMS was always found to be higher than from the other techniques, as a result of the negligible sensitivity of the FIGAERO-CIMS toward compounds without oxygen. Quantification of the SOA particle average  $\overline{OSc}$  was challenging, but all three techniques showed similar trends across systems. In the single precursor experiments, the initial concentration of precursors influences the average  $\overline{OSc}$  in the single  $\alpha$ -pinene experiment, but not in the single *o*-cresol experiment. In binary precursor systems, the injected isoprene affected the average  $\overline{OSc}$  in the presence of  $\alpha$ -pinene but the influence was more modest in the presence of *o*-cresol. The  $\overline{OSc}$  in the binary  $\alpha$ -pinene/isoprene mixture was lower than in the  $\alpha$ -pinene system although they have a similar trend in average  $\overline{OSc}$  with SOA mass concentration. This suggests that the isoprene has the potential to decrease the average  $\overline{OSc}$  by acting as an OH scavenger, resulting in suppression of the formation of low volatility and highly oxygenated organic compounds in a mixed system. The  $\overline{OSc}$  in the binary  $\alpha$ -pinene/*o*-cresol mixture was between those measured in the single precursor experiments, where that in the  $\alpha$ -pinene experiment was lower than in the *o*-cresol experiment, suggesting contributions to the  $\overline{OSc}$  from both precursors. In the ternary mixture, the  $\overline{OSc}$  was not dominated by any single precursor, with substantial contributions from products uniquely found in the mixture. These results implies that interactions between VOC products should be considered, to enable the level of chemical aging or oxidation of organic compounds understanding in ambient atmosphere.

## 1. Introduction

The formation and evolution of secondary organic aerosol (SOA) from mixtures of volatile organic compounds (VOCs) play an important role to understanding ambient organic aerosol (OA) composition. While early chamber studies predominantly investigated SOA formation from individual precursors (Lee et al., 2011; Winterhalter et al., 2003; Pandis et al., 1991; Hoffmann et al., 1997; Eddingsaas et al., 2012; Kroll et al., 2005a; Ahlberg et al., 2017; Pullinen et al., 2020; Kroll et al., 2005b), more recent research has shifted toward exploring multi-precursor systems (Han et al., 2025; Chen et al., 2025; Cui et al., 2024), reflecting the chemical complexity of the real atmosphere, where anthropogenic and biogenic VOCs coexist and interact. These interactions can significantly alter SOA yields, volatility distributions, and chemical composition, often through competition for oxidants or formation of cross-products.

~~For example, Mcfiggans et al. (2019) demonstrated that isoprene reduced SOA mass and yield by scavenging OH radicals and their derived products, thereby suppressing the formation of highly oxygenated molecules (HOMs) from  $\alpha$ -pinene oxidation and increasing the overall volatility of the mixture.emonstrated that a reduction of SOA mass and yield with isoprene acting as a scavenger toward OH radicals and its radical's products might contribute to scavenging the highly oxygenated  $\alpha$ -pinene products results in increasing the overall volatility of the products from mixture oxidation. In contrast,~~ However, more recent findings by Voliotis et al. (2022a) showed that although the addition of isoprene altered the chemical composition of the SOA and suppressed certain  $\alpha$ -pinene-derived products, the overall volatility distribution remained largely unchanged likely due to the formation of new products with comparable volatility distributions. Li et al. (2022) further demonstrated that isoprene can suppress SOA yields from anthropogenic aromatics (e.g., toluene, p-xylene) through OH scavenging, emphasizing the importance of VOC competition. Additionally, Zhao et al. (2025) highlighted mechanistic interactions in mixed biogenic systems, showing that in  $\alpha$ -pinene and limonene mixtures, limonene-derived RO<sub>2</sub> radicals and oxidation products facilitated the formation of cross-dimers, enhancing SOA yields. These findings highlighted the importance of the mechanistic interaction between the oxidation products of the precursor in understanding SOA formation in the presence of multiple VOCs.

Despite significant advances, the chemical characterization of SOA from mixed VOC systems remains challenging. OA in the ambient atmosphere comprises thousands of compounds, including hydrocarbons, alcohol, aldehydes and carboxylic acids, with a small fraction (~10-30%) of these capable of being characterised at a molecular level by current techniques (Hoffmann et al., 2011). Moreover, the chemical complexity of OA increases if there are multiple OA sources (both anthropogenic and biogenic sources) that contribute to OA formation. A current lack of detailed chemical characterisation of these organic species makes it difficult to track the OA sources, understand their atmospheric processes and mitigate their adverse impacts. The majority of ambient SOA is generated by oxidation of VOCs with the dominant prevailing oxidants, hydroxyl radicals (OH), ozone (O<sub>3</sub>) and nitrate radicals (NO<sub>3</sub>) with their relative contributions varying throughout the day and night, leading to low-volatility products that partition into the particle phase (Atkinson, 2004). As SOA ages, its composition evolves through multi-generational oxidation (Kroll et al., 2005a; Ahlberg et al., 2017; Pullinen et al., 2020)

A useful framework to describe this chemical evolution is the average carbon oxidation state ( $\overline{OSc}$ ), which increases with the extent of oxidation (Kroll et al. 2011). According to the valence rule, a simplified expression for the average  $\overline{OSc}$  of organic mixtures in terms of the molar oxygen to carbon (O/C) and hydrogen to carbon (H/C) ratios is shown in Equation 1.

$$\overline{OSc} = 2 * \frac{O}{C} - \frac{H}{C} \quad (1)$$

Changes in carbon oxidation state provide a valuable insight into the oxidation dynamics associated with the formation and evolution of ensemble SOA. For example, the  $\overline{OSc}$  generally increases by functionalisation, which can frequently occur in VOC oxidation leading to C-O bonds, for example, replacing C-H or unsaturated C-C bonds. An exception to this is when functionalisation leads to the addition of nitro groups forming a C-N bond, and  $\overline{OSc}$  remains the same. In contrast, the average  $\overline{OSc}$  remains unchanged by oligomerisation, which may occur after functionalisation and fragmentation reaction (Kroll et al., 2015). On the other hand, change in the average  $\overline{OSc}$  of particulate organic molecules is also associated with their volatility, which can strongly influence gas-particle partitioning, resulting in changes in the ensemble chemical

composition and increase of OA mass concentration. In general, the overall volatility will decrease with more functionalised molecules and increase with fragmentation (Daumit et al., 2013). Changes in  $\overline{OSc}$  and atomic ratios (H/C and O/C ratios) upon SOA mass loading can therefore be  
140 useful tools in identifying the key process in the atmospheric ageing of SOA.

In our chamber studies of SOA formation in mixtures of  $\alpha$ -pinene, isoprene and *o*-cresol, we have reported the chemical composition of SOA by offline ultra-high-performance liquid chromatography orbitrap mass spectrometry (Voliotis et al., 2022b; Shao et al., 2022a). Oxidation  
145 products from the high yield precursor,  $\alpha$ -pinene, dominated SOA in its mixtures, whilst isoprene derived compounds made a negligible contribution. Interactions in the oxidation of mixed precursors were found to lead to products uniquely found in the mixtures. In this study, we expand the investigation to report online measurements from the high resolution time-of-flight Aerodyne Aerosol Mass Spectrometers (HR-ToF-AMS) and Filter Inlet for Gases and AEROsols coupled to  
150 an Iodide high-resolution time of flight chemical ionisation mass spectrometer (FIGAERO-CIMS; Lee et al. (2014)) to measure the near real-time atomic ratios and derive the oxidation state of SOA during these experiments. The HR-ToF-AMS technique had been widely used for analysing the non-refractory aerosol chemical composition (Aiken et al., 2008; Shilling et al., 2009; Presto et al., 2009; Chhabra et al., 2010; Docherty et al., 2018) and can provide sensitive and online  
155 measurements of SOA elemental composition. The FIGAERO-CIMS was used to provide measurements of both gas-phase and particle-phase chemical constituents of organic aerosols in real time. Both instruments have limitations precluding molecular identification (electron impact ionisation in the HR-ToF-AMS leads to extensive fragmentation and the CIMS cannot resolve structural isomers or isobaric compounds (Lee et al., 2014)). Nevertheless, both online instruments  
160 can provide the time profile of atomic ratios of the SOA and derived average carbon oxidation state to add interpretation of the evolution of organic compounds to the offline measurement by ultra-high-performance liquid chromatography-high resolution mass spectrometry (UHPLC-HRMS).

165 The present study investigates the evolution of the average  $\overline{OSc}$  during SOA formation from single precursors and their mixture system, with a focus on linking the  $\overline{OSc}$  dynamics to underlying chemical mechanism. Specifically, five key questions were addressed and examined in this study:

i. How does  $\overline{OSc}$  vary with SOA mass loading to provide insights into volatility and aging process?

ii. How do different initial precursor reactivities influence  $\overline{OSc}$  evolution in single precursor experiments?

iii. How consistent are  $\overline{OSc}$  estimates across different analytical techniques, and what does the respective bias imply?

iv. How do the nitrogen-containing compounds affect the  $\overline{OSc}$  estimation, particularly in systems that contain abundant CHON products?

v. How does the mixing of precursors impact on the oxidation trajectories compared to the single precursor system, using  $\overline{OSc}$  as a diagnostic metric?

The present study aims to investigate the differences in  $\overline{OSc}$  in SOA formed from the photooxidation of single precursors and their mixtures. This is achieved by considering

i) the chemical mapping of identified SOA in FIGAERO-CIMS measurement and HR-ToF-AMS measurement;

ii) the relationship between precursors' initial concentration and extent of oxidation in SOA evolution in single precursors experiment;

iii) the dependence of the atomic ratios (O/C, H/C, and N/C ratios) and the extent of oxidation on SOA particle mass loading in single and mixture precursor systems

iv) the relative contributions to  $\overline{OSc}$  from the oxidation products of each precursor and whether any individual precursor controlled the average  $\overline{OSc}$  of SOA in mixed systems.

To answer these questions~~In order to achieve the objectives~~, a series of photochemical oxidation experiments were designed and conducted to produce SOA from the selected VOCs ( $\alpha$ -pinene, isoprene and *o*-Cresol) and their mixtures in the presence of neutral seed particles (ammonium sulphate) and NO<sub>x</sub>. The experimental program thereby included three single precursor experiments, three binary precursor mixtures and one ternary mixture of precursors. For studying the effect of the initial VOC concentration on the particle composition and carbon oxidation state of SOA evolution, here we also conduct single precursor experiments at half~~1/2~~ and third~~1/3~~ initial concentration (and hence reactivity towards the dominant oxidant in our experiments, the hydroxyl radical, OH). However, experiments with *o*-cresol at 1/3 reactivity and isoprene at 1/2 reactivity are

not reported as a result of technical difficulties. The HR-ToF-AMS and FIGAERO-CIMS continuously sampled and measured the SOA particles throughout the experiment and the entire chamber contents were flushed through a filter for collection of the aerosol at the end of the experiment for subsequent offline analysis by UHPLC-HRMS.

## 2. Materials and Methods

### 2.1. Experimental Procedure

The concept of iso-reactivity towards OH radicals was used to select the initial VOC concentrations in each experiment to enable comparable initial turnover of VOCs in the mixture with respect to OH radicals, such that the oxidation products from each VOCs would make comparable contributions at the chosen concentration and experimental conditions at the beginning of experiment. The injected mass of VOC precursors was calculated based solely on their reactivity with OH radicals (Atkinson, 2004), excluding their consumption by other oxidants (e.g., O<sub>3</sub>). Thirteen experimental conditions were planned, covering the  $\alpha$ -pinene, isoprene and *o*-cresol single precursor experiments (~~each at full, half and third reactivity~~) (~~each at full,  $\frac{1}{2}$  and  $\frac{1}{3}$  reactivity~~) respectively, binary  $\alpha$ -pinene / isoprene,  $\alpha$ -pinene / *o*-cresol and *o*-cresol / isoprene mixtures and their ternary mixture. Initial concentrations of each VOC in the binary and ternary mixtures were the same as the initial concentration in the  ~~$\frac{1}{2}$ -half~~ and  ~~$\frac{1}{3}$ -third~~ reactivity individual VOC experiments respectively, ensuring comparable initial reactivity toward OH in all systems.

As described in Shao et al. (2022b), a “pre-experiment” program and a “post-experiment” were conducted prior to and after each experiment. These two procedures consist of multiple auto fill/flush cycle with high flow rate ( $\sim 3 \text{ m}^3 \text{ min}^{-1}$ ) with purified air to condition and remove the unwanted contaminants in the chamber bag. A water condensation particle counter (WCPC; TSI 3786), O<sub>3</sub> analyser, (Thermo Electron Corporation model 49C), NO-NO<sub>2</sub>-NO<sub>x</sub> analyser (Thermo Electron Corporation model 42i) were used to monitor residual gas and particles in the chamber during the “pre-experiment”, to ensure their concentrations were close to zero in the bag prior to chamber background procedure. The “chamber background” was conducted for approximately 1h, while collection of data from the chamber in the dark, which the chamber and all instrumentation are all stabilized. An “experimental background” procedure was conducted in the next stage to

establish the baseline contamination level in the chamber. This comprised continuous measurement after injecting VOC(s), NO<sub>x</sub>, and seed particles sequentially and leaving the chamber to stabilise for an hour under dark condition. All the subsequent analysis presented in this work has the “chamber background” and “experimental background” subtracted. The baseline of clean background and the experimental background were used to correct experimental data (See Supporting information Section 1). Actinometry and off-gassing experiments were performed regularly during our campaign to monitor the condition and cleanliness of the chamber bag.

The duration of each experiment was nominally 6 hours after initial illumination, under similar controlled environmental conditions (RH:50±5% and T:24±2 °C). The average OH concentration during illumination was estimated from the decay rates of solely OH-reactive VOCs (e.g., *o*-Cresol), yielding a concentration of approximately  $1 \times 10^6$  molecules cm<sup>-3</sup>. This OH source arose from O<sub>3</sub> generated via NO<sub>2</sub> photolysis, which was further photolysed in the moist chamber atmosphere. The summary of the initial conditions of the reported experiments ~~awere~~ presented in table 1 (noting the lack of ~~third~~<sup>1/3</sup> reactivity *o*-cresol and ~~half~~<sup>1/2</sup> reactivity- isoprene owing to technical difficulties). To enhance confidence in the validity of our results and to address technical issues caused by occasional instrument failures, repeat experiments were conducted for selected single-precursor systems (both full and half reactivity), as well as for the binary and ternary mixture systems. However, this study presents results from only one experiment per system, ~~withas~~ previous studies by Voliotis et al. (2021, 2022b) and Shao et al. (2022a) ~~have~~ already demonstratinged good agreement across repeated experiments in terms of maximum SOA mass, volatility distribution, and chemical composition within each system. The particulate products were collected at the end of each experiment, flushing the entire chamber contents through a pre-fired quartz filter (heating in a furnace at 550 °C for 5.5 hours), which was subsequently wrapped in foil and refrigerated at -18 degrees.

Table 1: Summary of the initial conditions of experiments.

Exp. no.	Exp. Type	Precursors Reactivity	VOC	NO <sub>x</sub> (ppb)	VOC (ppb)	VOC/ NO <sub>x</sub>	Seed (μg m <sup>-3</sup> )
a	Single	Full	α-pinene	40	309	7.7	72.6
b		Half	α-pinene	26	155	6.0	45.7
c		Third	α-pinene	18	103	5.7	51.0



d		Full	<i>o</i> -cresol	44	400	9.1	47.8
e		Half	<i>o</i> -cresol	40	200	5.0	51.3
f		Full	isoprene	23	164	7.1	-
g		Third	isoprene	15	55	3.9	42.2
h	<b>Binary</b>	Full	<i>o</i> -cresol/isoprene	34	282 (200/82)	8.3	49.6
i		Full	$\alpha$ -pinene/ <i>o</i> -cresol	30	355 (155/200)	11.8	57
j		Full	$\alpha$ -pinene/isoprene	39	237 (155/82)	6.1	62.0
k	<b>Ternary</b>	Full	$\alpha$ -pinene/ <i>o</i> -cresol/isoprene	78	291 (103/133/55)	3.7	45.8

## 2.2. Instrumentation

### 2.2.1. Manchester Aerosol Chamber

All experiments were conducted in the Manchester Aerosol Chamber (MAC; Shao et al. (2022b)).

Briefly, the MAC operates as a batch reactor and consists of 18m<sup>3</sup> volume Teflon FEP bag suspended by three rectangular extruded aluminium frames, housed in an air-conditioned enclosure. The enclosure is covered by reflective mylar material and is illuminated with two 6 kW Xenon arc lamps (XBO 6000 W/HSLA OFR, Osram) and a bank of halogen lamps (Solux 50 W/4700 K, Solux MR16, USA) with an intensity corresponding to a photolysis rate of NO<sub>2</sub> (jNO<sub>2</sub>) around 1.83x10<sup>-3</sup> s<sup>-1</sup> through the entire experimental campaign. Conditioned air was introduced between the bag and the enclosure to maintain a constant chamber temperature throughout the experiment. Additionally, active water was used to cooling of the mounting bars of the halogen lamps and of the filter in front of the arc lamps to remove the unwanted heat from the lamps. Relative humidity (RH) and temperature (T) are controlled by the humidifier and by the air conditioning that couple with the chamber. RH and T were continuously monitored by the dewpoint hygrometer and several thermocouples and resistance probes during the experiment. Liquid VOCs ( $\alpha$ -pinene, isoprene and *o*-cresol; Sigma Aldrich, GC grade  $\geq 99.99\%$  purity) were introduced into chamber through injection into a heated glass bulb for vaporization and subsequently flushed into the chamber with purified N<sub>2</sub> (electronic capture device-grade nitrogen stream; purity  $\geq 99.998\%$ ). A custom-made cylinder (10% v/v) containing NO<sub>x</sub> was used for NO<sub>2</sub> injection into the MAC in ECD N<sub>2</sub> as carrier gas. A Topaz model ATM 230 aerosol generator were

used to produce ammonium sulphate seed particles by atomization from ammonium sulphate solution (Puratonic, 99.999% purity).

### 2.2.2. Online Measurement

The NO-NO<sub>2</sub>-NO<sub>x</sub> and O<sub>3</sub> analysers were used to measure the NO<sub>2</sub> and O<sub>3</sub> gas concentration throughout the experiments. A semi-continuous gas chromatograph (6850 Agilent) coupled to a mass spectrometer (5975C Agilent; hereafter GC-MS) with a thermal desorption unit (Markes TT-24/7) was employed to monitor the time profile of VOC precursor decay. An Aerodyne high-resolution time-of-flight aerosol mass spectrometer (HR-ToF-AMS, Aerodyne Research Inc., USA) was used to measure organic mass loading and characterize the composition of non-refractory organic particles. The HR-ToF-AMS instrument was calibrated by using monodisperse (350nm) ammonium nitrate and ammonium sulphate particle prior to and after to the experimental program, referring to the standard protocol in Jayne et al. (2000) and Jimenez et al. (2003). The instrument operated in “V mode” during experiments and ran in mass spectra (MS) and particle-time-of-flight (PToF) sub-modes for equal time periods (30s each section). The HR-ToF-AMS data were processed in Igor Pro 7.08 (Wavemeterics.Inc.) using the standard ToF-AMS analysis toolkit (version 1.21) for both unit mass resolution (UMR) and high resolution (HR) analyses. The average ionisation efficiency of nitrate (IE=9.38 x 10<sup>8</sup>), the specific relative ionisation efficiencies (RIE) for NH<sub>4</sub><sup>+</sup> (3.57 ± 0.02) and SO<sub>4</sub><sup>2-</sup> (1.28 ± 0.01) from calibration, and the default RIE from Alfarra et al. (2004) of all organic compounds (RIE=1.4) were all applied in the UMR and HR analysis. HR mass spectra was fitted using the method of DeCearlo et al. (2006) and analysed using the ToF-AMS analysis software that reported in D.-Sueper et al. (2020). The ion fitting process for high resolution mass spectra in our analysis refers to the supporting information in Hildebrandt et al. (2011), since this is critical in the determination of the atomic ratio (O/C), and (H/C) of non-refractory organic material.

The operation of the time-of-flight chemical ionisation mass spectrometer with iodide ionisation coupled with a filter inlet for gases and aerosols (FIGAERO-CIMS ; Lopez-Hilfiker et al. (2014)) was described in Voliotis et al. (2021). Briefly, the particles were sampled for 30 mins to the PTFE filter (Zefluor, 2.0 µm pore size) at 1 sL min<sup>-1</sup>, following by 33 mins thermal desorption (15-min temperature ramp to 200 °C, 10 mins holding time and 8 mins

cooling down to room temperature) with ultra-high purity N<sub>2</sub> as carrier gas. The instrument was run in negative-ion mode by producing I<sup>-</sup> reagent ion generated using polonium-210 ionisation source to ionize methyl iodide (CH<sub>3</sub>I). The I<sup>-</sup> reagent ions enter the ion molecule reaction region (IMR) with N<sub>2</sub> (ultra-high purity) as carrier gas. An “instrument background” procedure for the particle phase measurements was conducted in all the experiments for subtraction from the measurements. The FIGAERO-CIMS data were processed by using the Tofware package in Igor Pro 7.0.8 (version. 3.2.1., Wavemetrics©) (Stark et al., 2015) for peak identification. A data set of assigned molecular formula of detected compounds were produced, allowing subsequent determination of the H/C and O/C ratios.

### 2.2.3. Offline Measurement

Ultra-performance liquid chromatography ultra-high resolution mass spectrometry (Dionex 3000, Orbitrap QExactive, ThermoFisher Scientific) was employed for analysing the filter sampled particulate. A detailed description of the instruments, experimental set-up and data processing methodology can be found on Shao et al. (2022a) and Pereira et al. (2021). Briefly, the preparation of sample solution is as follows:

1) Filter samples were dissolved in 4 mL of LCMS-grade methanol, left to stand for 2 hours at ambient temperature, and then extracted using sonication for 30 minutes (Fisher Scientific FB15051).

2) 0.22 µm pore size PDVF filter (Fisher Scientific) and BD PlasticPak syringe (Fisher Scientific) were used for filtering the sample solution, followed by adding further 1 ml methanol on the dry filter for the second extraction of samples with the same method.

3) The extracted solution was evaporated to dryness using a solvent evaporator (Biotage) under specified temperature (36 °C) and pressure (8 mbar) conditions. The evaporation step may result in the partial loss of the most volatile SOA components; however, most LCMS detectable species are of low-volatility and thus retained under these conditions.

4) The extract residual was re-dissolved in 1 ml solvent that consists of LCMS optimal grade water and methanol in a ratio of 9:1.

Once the sample solutions were prepared, they were injected into the UHPLC-HRMS 0.3 ml/min with 2  $\mu$ l volume by autosampler held at 4 °C. The mass spectrometer was mass calibrated using ESI positive and negative ion calibration solutions (Pierce, Thermo Scientific) prior to sample analysis. The sample solution was passed through a reverse-phase C18 column (Accucore, Thermo  
350 Fisher Scientific) 100 mm long  $\times$  2.1 mm wide and with 2.6  $\mu$ m particle size, with temperature held at 40°C. The mobile phase was composed of (A) LCMS optimal grade water (Sigma Aldrich) and (B) methanol (LC-MS Optimal grade, Fisher Scientific) that both contain 0.1% (v/v) formic acid (Sigma Aldrich, 99% purity). The gradient elution started at 90% (A) with a 1-minute post-injection hold, decreased to 10% (A) over 26 minutes, returned to the initial mobile phase at 28  
355 minutes, and ended with a 2-minute re-equilibration. In this instrument, electrospray ionisation (ESI, 35 eV) was performed for both positive and negative mode to charge the organic compounds in a range of m/z 80 to m/z 750. High-energy collisional dissociation from tandem mass spectrometry (MS<sup>2</sup>) was used to generate ion fragments for subsequent mass analyser detection.

~~The resulting product ion spectra were then used to support structural characterisation and isomer  
360 identification of the compounds. Thus, produced product ion spectrum, to inform the compound's structural characterisation and isomer identification.~~ Analysis of extracted solvent (water: methanol = 9:1) and pre-conditioned bank filter was also performed with the same procedure for subtraction from the measurements to ensure exclusion of baseline noise and artefacts from sample preparation.

365 The data was processed by an automated methodology for non-targeted composition of small molecules (Pereira et al. (2021)). This approach guided the peak identification and molecular formula assignment for detected compounds, enabling calculation of the signal weighted  $\overline{OSc}$ , O/C, H/C and H/C for each system.

### 370 2.3. Estimation of average carbon oxidation state ( $\overline{OSc}$ )

For compounds that contain only carbon, hydrogen and oxygen (designated “CHO” compounds), the average  $\overline{OSc}$  was straightforwardly determined using atomic ratios O/C and H/C using  
375 equation 1,  $\overline{OSc} = 2 \times \text{O/C} - \text{H/C}$ , in analysis of data from all MS techniques.

For compounds that additionally contain nitrogen (“CHON” compounds), it is assumed that the nitrogen would exist as nitrate with  $\overline{OS}_N = +5$  if there are 3 or more oxygen atoms in the molecule

and as nitrite with  $\overline{OS}_N = +3$  if there are fewer than 3 oxygen atoms. For CHON compounds, the  $\overline{OS}_C$  is therefore calculated using equation (2) where the H, C, O and N are determined from the FIGAERO-CIMS and UHPLC-HRMS signal.

$$\overline{OS}_C = 2 * \frac{O}{C} - \frac{H}{C} - (\overline{OS}_N * \frac{N}{C}) \quad (2)$$

Where N/C corresponding to nitrogen-to-carbon ratios,  $\overline{OS}_N = 3$  if  $nO < 3$ ; or  $\overline{OS}_N = 5$  if  $nO \geq 3$ .

The signal-weighted average  $\overline{OS}_C$  determined by equation (2) will be presented in section 3 and referred to as “accounting for  $\overline{OS}_N$ ”. The HR-ToF-MS is unable to provide molecular information,

but provides total particle ensemble C, H and O from the HR mass defect. However, retrieval of mass defect with sufficient accuracy to attribute the N-containing compounds at the resolution of the instrument is too challenging to be considered robust. The calculated  $\overline{OS}_C$  from HR-ToF-AMS data uses only C, H and O and uses equation 1 (i.e. implicitly not accounting for organic nitrogen in any CHON compounds present). For comparison with the HR-ToF-AMS -calculated  $\overline{OS}_C$ , the average  $\overline{OS}_C$  for CHON compounds measured by the FIGAERO-CIMS and UHPLC-HRMS technique has also been calculated ignoring the N and using equation (1), and this referred to as “not accounting for  $\overline{OS}_N$ ”. in section 3

Strictly, the estimation of average carbon oxidation state should account for the oxidation state of sulphur ( $\overline{OS}_S$ ) in any sulphur-containing compounds (CHOS and CHONS compounds) in the particles. Given the challenges associated with the quantification of S-containing compounds in FIGAERO-CIMS technique (Xu et al., 2016; D'ambro et al., 2019), this study does not consider the contribution of  $\overline{OS}_S$  in  $\overline{OS}_C$  calculation. It was also shown by Du et al. (2021) that the influence of heteroatom S or NS on  $\overline{OS}_C$  calculation would be negligible as a result of their low fractional abundance the in UHPLC-HRMS measurements (see also Shao et al. 2022).

In this study, the average  $\overline{OS}_C$  reported from a "representative experiment," where only the compounds found in all replicate experiments can be confidently attributed to this particular system in both UHPLC-HRMS and FIGAERO-CIMS analyses. The HR-ToF-AMS measurements were selected from the same 'representative experiment' as the UHPLC-HRMS and FIGAERO-CIMS analyses.

### 3. Results

#### 3.1. 3.1. Average $\overline{OSc}$ Evolution of single precursor experiments (with $\overline{OS_N}$ correction)

##### ~~3.1. $\overline{OSc}$ of Particles in Single VOC experiment at various reactivity levels~~

Figure 1 shows the average  $\overline{OSc}$  as a function of SOA mass concentration from single  $\alpha$ -pinene and *o*-Cresol experiments with different initial reactivities respectively, derived from FIGAERO-CIMS and UHPLC-HRMS measurements. All values shown here include the  $\overline{OS_N}$  correction.

For the single  $\alpha$ -pinene system (Fig. 1a), the average  $\overline{OSc}$  estimated from FIGAERO-CIMS decreased with increasing SOA mass across all three reactivity levels. The magnitude of this decrease was similar among experiments. In the third reactivity experiment (lowest precursor concentration), the average  $\overline{OSc}$  declined from  $-0.24$  to  $-0.46$ , while in the half reactivity experiment it decreased from  $-0.31$  to  $-0.51$ , and in the full reactivity experiment from  $-0.35$  to  $-0.57$ .

The UHPLC-HRMS results in negative ionisation mode showing comparable trends. In negative ionisation mode, the endpoint average  $\overline{OSc}$  values were  $-0.45$  for the third reactivity  $\alpha$ -pinene experiment, which is higher than that a half reactivity ( $\overline{OSc} = -0.61$ ) and full reactivity ( $\overline{OSc} = -0.58$ ) experiment. In positive ionisation mode, the half and full reactivity experiments gave similar average  $\overline{OSc}$  magnitude (around  $-0.95$ ), which were about  $0.26$  higher than the third reactivity experiment.

For the *o*-Cresol system (Fig. 1b), the average  $\overline{OSc}$  from FIGAERO-CIMS decreased with increasing SOA mass in both reactivity experiments. In the full reactivity experiment, the average  $\overline{OSc}$  declined from  $0.12$  to  $-0.26$ , while in the half reactivity experiment it decreased from  $0.09$  to  $-0.37$ . At the very beginning of the half reactivity experiment, the first point shows a lower  $\overline{OSc}$  of about  $-0.25$ , but this corresponds to exceptionally low SOA mass loadings.

The UHPLC-HRMS results show similar behaviour. In negative ionisation mode, the full and half reactivity experiments gave comparable endpoint values of around  $-0.55$ . In positive ionisation mode, however, the half-reactivity experiment has a higher  $\overline{OSc}$  ( $-0.48$ ) than the full reactivity experiment ( $-0.66$ ).

Figure 1 shows the average carbon oxidation state of SOA against SOA mass concentration from the single precursor VOC experiments ( $\alpha$ -pinene (panel a and b) and *o*-cresol (panel c and d))

conducted at different initial reactivity level. Panels (a) and (c) show the average  $\overline{OSc}$  of SOA accounting for  $\overline{OS_{\text{M}}}$ , and (b) and (d) without accounting for  $\overline{OS_{\text{M}}}$  of SOA detected by different MS techniques.

445 In the single precursor  $\alpha$ -pinene experiments, the average  $\overline{OSc}$  accounting for  $\overline{OS_{\text{M}}}$  as a function of mass loading showed small differences between the three initial concentration experiments in FIGAERO-CIMS data ( $\overline{OSc}$  at  $\frac{1}{3}$  reactivity decreased from 0.24 to 0.46 across the 6-hour experimental period and was very slightly higher than at  $\frac{1}{2}$  reactivity ( $\overline{OSc}$  = 0.31 to 0.51) and full reactivity ( $\overline{OSc}$  = 0.35 to 0.57) (Fig. 1a). Comparably, the average  $\overline{OSc}$  in the  $\frac{1}{3}$  reactivity  
450 single precursor  $\alpha$ -pinene experiment was 0.45 in negative ionisation mode in UHPLC-HRMS, which is slightly higher than that at  $\frac{1}{2}$  reactivity ( $\overline{OSc}$  = 0.61) and full reactivity ( $\overline{OSc}$  = 0.58) experiment. In contrast, in positive ionisation mode, the average  $\overline{OSc}$  in the  $\frac{1}{2}$  reactivity system is comparable to that in the full reactivity system ( $\overline{OSc}$   $\approx$  0.95) and is approximately 0.26 higher than  $\overline{OSc}$  in the  $\frac{1}{3}$  reactivity system (Fig. 1a).

455 Fig. 1b shows the average  $\overline{OSc}$  not accounting for  $\overline{OS_{\text{M}}}$  against particle mass concentration enabling comparison against the HR-ToF-AMS data in the  $\alpha$ -pinene experiments. The average  $\overline{OSc}$  derived from HR-ToF-AMS showed significant differences between three initial reactivity experiments. Fig. 1b shows that the HR-ToF-AMS is able to estimate  $\overline{OSc}$  at lower total particle mass during the rapid early growth phase of the experiments compared to the other two techniques, before the first FIGAERO sample is collected. First, it is clear that the total SOA mass concentration trajectory is markedly different for the various initial  $\alpha$ -pinene concentration (Fig. 1b). Also, the  $\frac{1}{2}$  reactivity system has the highest average  $\overline{OSc}$  from 0.99 to 0.31 compared to full reactivity ( $\overline{OSc}$  = 1.68 to 0.39) and  $\frac{1}{3}$  reactivity ( $\overline{OSc}$  = 2.51 to 0.66) system as function  
460 of SOA mass concentration. The average  $\overline{OSc}$  of both full and  $\frac{1}{2}$  reactivity systems showed upward trend first, followed by reduction during SOA evolution. The average  $\overline{OSc}$  was increasing continuously until the end of the experiment in  $\frac{1}{3}$  reactivity system. The average  $\overline{OSc}$  values derived from FIGAERO-CIMS in Fig. 1b each show higher values than those from the HR-ToF-AMS. The  $\overline{OSc}$  from FIGAERO-CIMS is comparable between full reactivity ( $\overline{OSc}$  = 0.17 to  
465 0.40) and  $\frac{1}{2}$  reactivity systems ( $\overline{OSc}$  = 0.17 to 0.32). Both are slightly lower than the  $\frac{1}{3}$  reactivity  
470

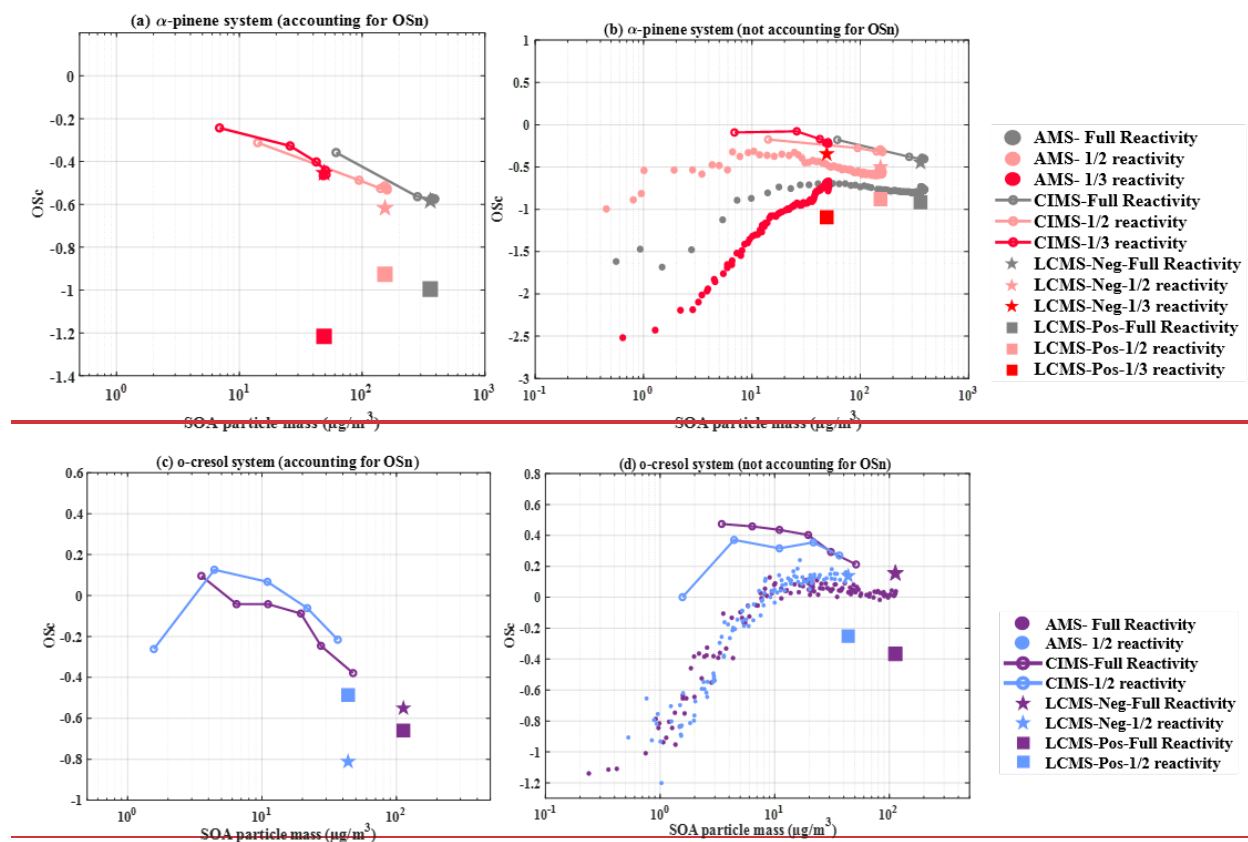
system ( $\overline{OSc} = -0.07$  to  $-0.22$ ), which is opposite to the HR-ToF-AMS trend. The UHPLC-HRMS derived average  $\overline{OSc}$  not accounting for  $\overline{OS_N}$  from the  $\frac{1}{2}$  reactivity experiment is slightly higher ( $-0.34$ ) in negative ionisation mode, and lower ( $-0.19$ ) in positive ionisation mode than that from the other two experiments, with the negative ionisation values all comparable to those from the FIGAERO-CIMS. As must be the case given the presence of nitrogen atom in the spectra, the average  $\overline{OSc}$  accounting for  $\overline{OS_N}$  is lower value than when not accounting for  $\overline{OS_N}$  derived from both FIGAERO-CIMS and UHPLC-HRMS (Fig. 1a and 1b).

For single precursor *o*-cresol experiments, the FIGAERO-CIMS derived average  $\overline{OSc}$  accounting for  $\overline{OS_N}$  decreased with increasing SOA mass concentration in both the full and  $\frac{1}{2}$  reactivity experiments, with the extent of reduction being fairly similar (from  $0.12$  to  $-0.26$  in the  $\frac{1}{2}$  reactivity experiment and from  $0.09$  to  $-0.37$  in the full reactivity experiment), as shown in Fig. 1c. Meanwhile, the full reactivity experiment showed a higher UHPLC-HRMS derived  $\overline{OSc}$  ( $-0.55$ ) than the  $\frac{1}{2}$  reactivity experiment ( $-0.81$ ) in negative ionisation mode, but with an opposite trend in positive ionisation mode (Fig. 1c). The difference in average  $\overline{OSc}$  when accounting for  $\overline{OS_N}$  versus not accounting for it was larger in the half reactivity experiment ( $\delta \overline{OSc} = 0.95$ ) than in the full reactivity experiment ( $\delta \overline{OSc} = 0.70$ ), suggesting a greater relative contribution of nitrogen-containing compounds under lower precursor conditions. When not accounting for  $\overline{OS_N}$ , the HR-ToF-MS derived  $\overline{OSc}$  shows a similar increasing trend with SOA particle mass at each initial concentration, with comparable values ranging from  $-1.20$  to  $0.24$  as shown in Fig. 1d), with the only difference being that the full reactivity experiment showed slight decrease in  $\overline{OSc}$  after SOA mass concentration reached its peak at around  $10 \mu\text{g m}^{-3}$ .

As with the  $\alpha$ -pinene experiments, the FIGAERO-CIMS derived average  $\overline{OSc}$  were comparable between initial concentration *o*-cresol experiments and higher than the HR-ToF-AMS derived  $\overline{OSc}$ . The  $\overline{OSc}$  reduced with increasing particulate mass concentration from ( $\sim 0.4$  to  $0$ ). Negative ionisation mode average  $\overline{OSc}$  from UHPLC-HRMS measurements at both initial concentrations were comparable at  $\sim 0.14$  (Fig. 1d). In positive mode, the average  $\overline{OSc}$  at the higher concentration was  $-0.36$ ,  $0.11$  lower than the lower concentration value.



500 The SOA particle mass yield (and hence particle mass loading) in the single VOC isoprene experiment was so close to zero that it was not possible to provide meaningful data on changes in composition, as noted in Voliotis et al., (2022a, 2022b).



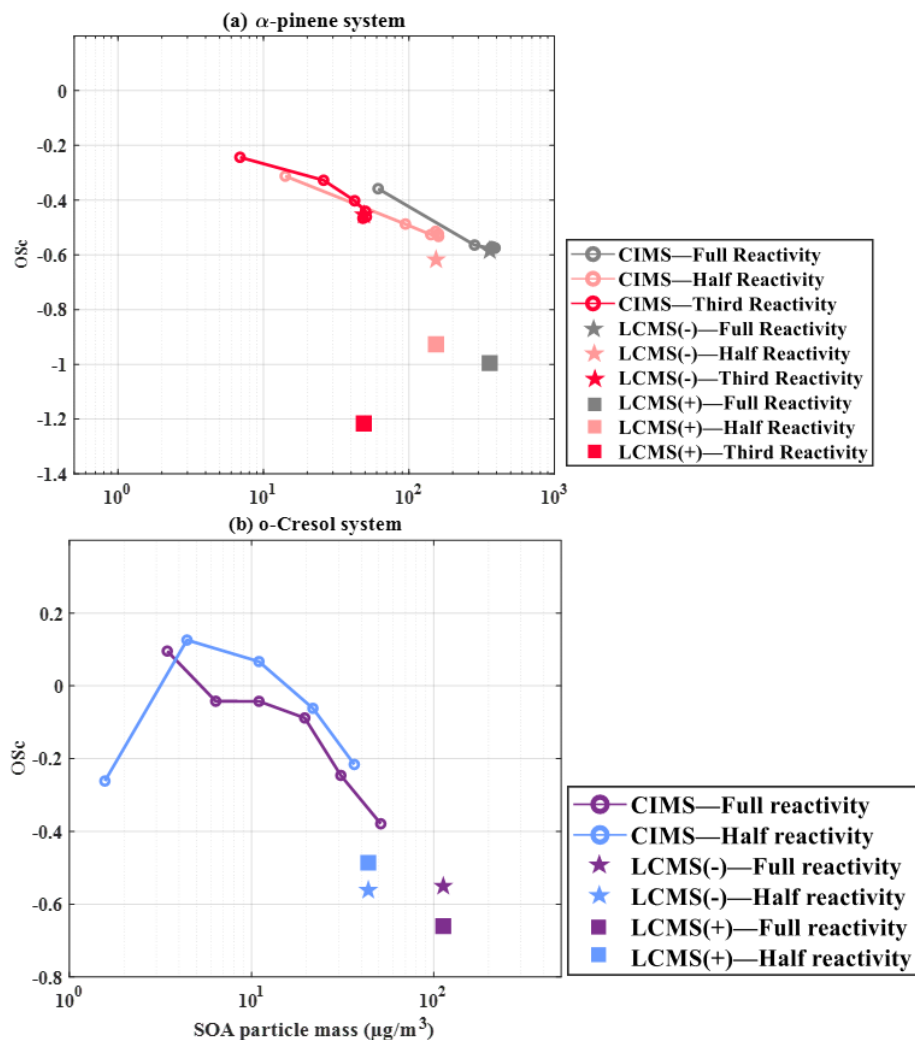


Figure 1 : Average  $\overline{OSc}$  (with  $\overline{OS_N}$  correction) estimated from the FIGAERO-CIMS (Lines) and UHPLC-HRMS (symbols; negative ion mode = stars, positive ion mode = squares) as a function of SOA mass. (a) Single  $\alpha$ -pinene experiments with three initial reactivity: (b) Single *o*-Cresol experiments with two initial reactivity

Figure 1: Average carbon oxidation state as function of SOA mass concentration of products detected by the HR-ToF-AMS, FIGAERO-CIMS, and UHPLC-HRMS measurements (Negative Ionization Mode (Neg) and Positive ionization mode (Pos)) in the single precursor  $\alpha$ -pinene and *o*-cresol systems. a) and c) accounting for  $\overline{OS_N}$ . b) and d) not accounting for  $\overline{OS_N}$ .

### 3.2. Average $\overline{OSc}$ Evolution of single precursor experiments (without $\overline{OS_N}$ correction)

Figure 2 shows the evolution of  $\overline{OSc}$  as a function of SOA mass in single  $\alpha$ -pinene and *o*-Cresol experiments across different reactivities, estimated using HR-ToF-AMS, FIGAERO-CIMS, and UHPLC-HRMS measurement. It is important to note that the average  $\overline{OSc}$  value in Figure 2 do not include the  $\overline{OS_N}$  correction term.

In the single  $\alpha$ -pinene experiments (Fig. 2a), the HR-ToF-AMS is able to estimate  $\overline{OSc}$  at lower particle mass during the rapid early growth phase compared with the other two techniques. The half reactivity experiment exhibits the highest average  $\overline{OSc}$  (-1 to -0.5), followed by the full reactivity experiment ( $\overline{OSc}$  : -1.6 to -0.7) while the third reactivity experiment remains lowest ( $\overline{OSc}$ : -2.48 to -0.68). In both the full and half reactivity experiments, the average  $\overline{OSc}$  initially increases and then declines as SOA mass builds, whereas in the third reactivity experiment it increases continuously until the end of the experiment. By contrast, FIGAERO-CIMS consistently reports higher  $\overline{OSc}$  than the AMS across all three experiments. For FIGAERO-CIMS, the full ( $\overline{OSc}$ : -0.17 to -0.40) and half reactivity ( $\overline{OSc}$ : -0.17 to -0.32) experiments give comparable values, both slightly lower than the third reactivity experiment ( $\overline{OSc}$ : -0.07 to -0.22), which is the opposite trend to that observed with AMS measurement. The UHPLC-HRMS results also align more closely with FIGAERO-CIMS, with the third reactivity experiment giving  $\overline{OSc}$  of -0.34 in negative ionisation mode and -0.19 in positive ionisation mode, with the negative ionisation values all comparable to the FIGAERO-CIMS estimates.

For the single *o*-Cresol experiments, the HR-ToF-AMS derived average  $\overline{OSc}$  shows a broadly increasing trend with SOA mass under both full and half reactivity conditions, with magnitudes ranging from -1.2 to 0.2 (Fig. 2b). The two experiments are generally comparable, except that the full reactivity experiment exhibits a slight decline in average  $\overline{OSc}$  once SOA mass peaks at  $\sim 10 \mu\text{g m}^{-3}$ . In addition, FIGAERO-CIMS estimation showed higher average  $\overline{OSc}$  than HR-ToF-AMS measurement, with comparable values between the two reactivity conditions, and a clear decrease from  $\sim 0.4$  to  $\sim 0$  as particle mass increases. The UHPLC-HRMS measurements also show similar behaviour across reactivities. In negative ionisation mode, the average  $\overline{OSc}$  is  $\sim 0.14$  in both

experiments, while in positive mode the full reactivity experiment gives  $-0.36$ , about  $0.11$  lower than the half reactivity experiment.

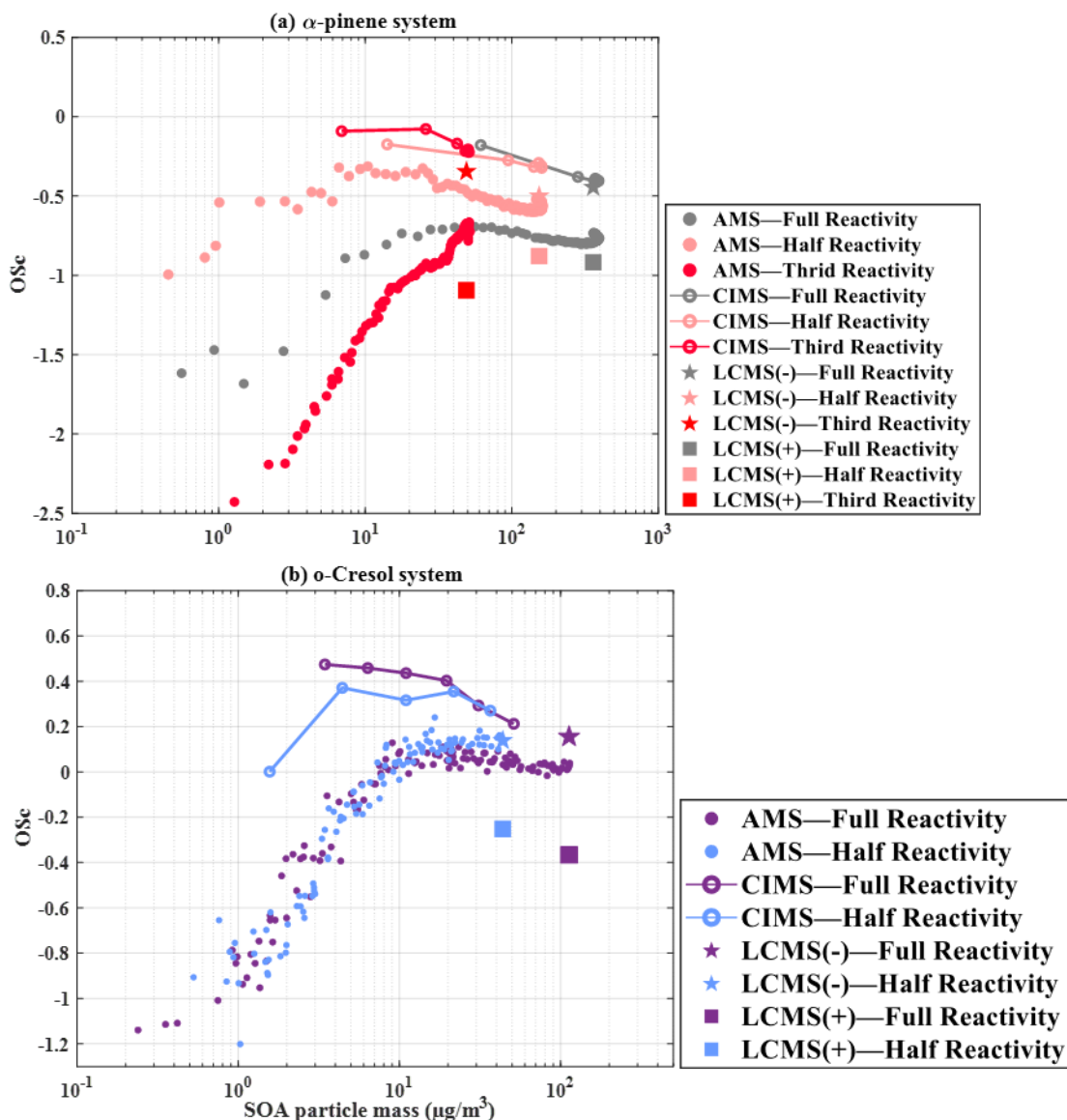


Figure 2. Average  $\overline{OSc}$  (without  $\overline{OS_N}$  correction) as a function of SOA particle mass for single-precursor systems: (a)  $\alpha$ -pinene with three initial reactivity and (b) *o*-Cresol with two initial reactivity, obtained from HR-ToF-AMS (Dots), FIGAERO-CIMS (Lines), and UHPLC-HRMS (symbols; negative ion mode = stars, positive ion mode = squares).

### 3.2. $\overline{OSc}$ , O/C and H/C ratios of SOA Particles in mixtures accounting for $\overline{OS_{\text{FF}}}$

This section compares the average carbon oxidation state and atomic ratios of particles derived from FIGAERO-CIMS and UHPLC-HRMS data from mixed precursors systems with reference to their corresponding single precursors experiments. The average carbon oxidation state presented in this section accounts for the nitrogen present in all systems (though not the sulphur) see section 2.4, and excludes HR-ToF-AMS data, owing to the challenges with accounting for  $\overline{OS_N}$ .

#### (a) $\alpha$ -pinene & isoprene binary system

Figure 2 shows the atomic ratios (O/C, H/C and N/C) and average carbon oxidation state  $\overline{OS_C}$  of the evolving SOA particles in binary  $\alpha$ -pinene/isoprene mixture, individual  $\frac{1}{2}$  reactivity  $\alpha$ -pinene and full reactivity isoprene experiments (noting the unavailability of data for lower concentration isoprene experiments). As might be expected from its very low (near negligible) mass contribution (below the background chamber concentration ( $<1\mu\text{g m}^{-3}$ )), whilst the particle produced in the isoprene experiment appear quite highly oxidized in comparison to those from  $\alpha$ -pinene, the isoprene products appear to have a minor effect on the carbon oxidation state and atomic ratios in binary  $\alpha$ -pinene / isoprene system.

Panel a) shows the FIGAERO-CIMS average  $\overline{OS_C}$  in  $\frac{1}{2}$  reactivity  $\alpha$ -pinene experiments have a similar declining trend (from -0.31 to -0.51 through the experiment) as that in the binary mixture (from -0.42 to -0.65), though being slightly more oxidised. As shown in panels b) and c), the mixture and individual  $\alpha$ -pinene experiments showed comparable O/C ( $\sim 0.63$  and  $0.60$ ) and H/C ratios (H/C  $\sim 1.45$  to  $1.55$ ). The N/C ratios increased as function of SOA mass concentration in both experiments, with more N in the mixture (N/C increasing from  $0.03$  to  $0.08$ ) than in the individual  $\alpha$ -pinene experiment (N/C =  $0.03$  to  $0.04$ ) (panel d)).

The UHPLC-HRMS  $\overline{OS_C}$  and element atomic ratios (O/C, H/C and N/C) are comparable in negative ionisation modes in the mixture and individual  $\alpha$ -pinene experiment (and similar to the FIGAERO-CIMS average  $\overline{OS_C}$ .  $\overline{OS_C}$  in the individual  $\alpha$ -pinene experiment in positive ionisation mode is slightly ( $0.1$ ) higher ( $-0.92$ ) than in the mixture (Fig.2a), reflecting a higher O/C and lower N/C. The values from the last FIGAERO-CIMS measurements are similar to those from the

UHPLC-HRMS negative ionisation measurements, both are higher than those from positive ionisation mode.

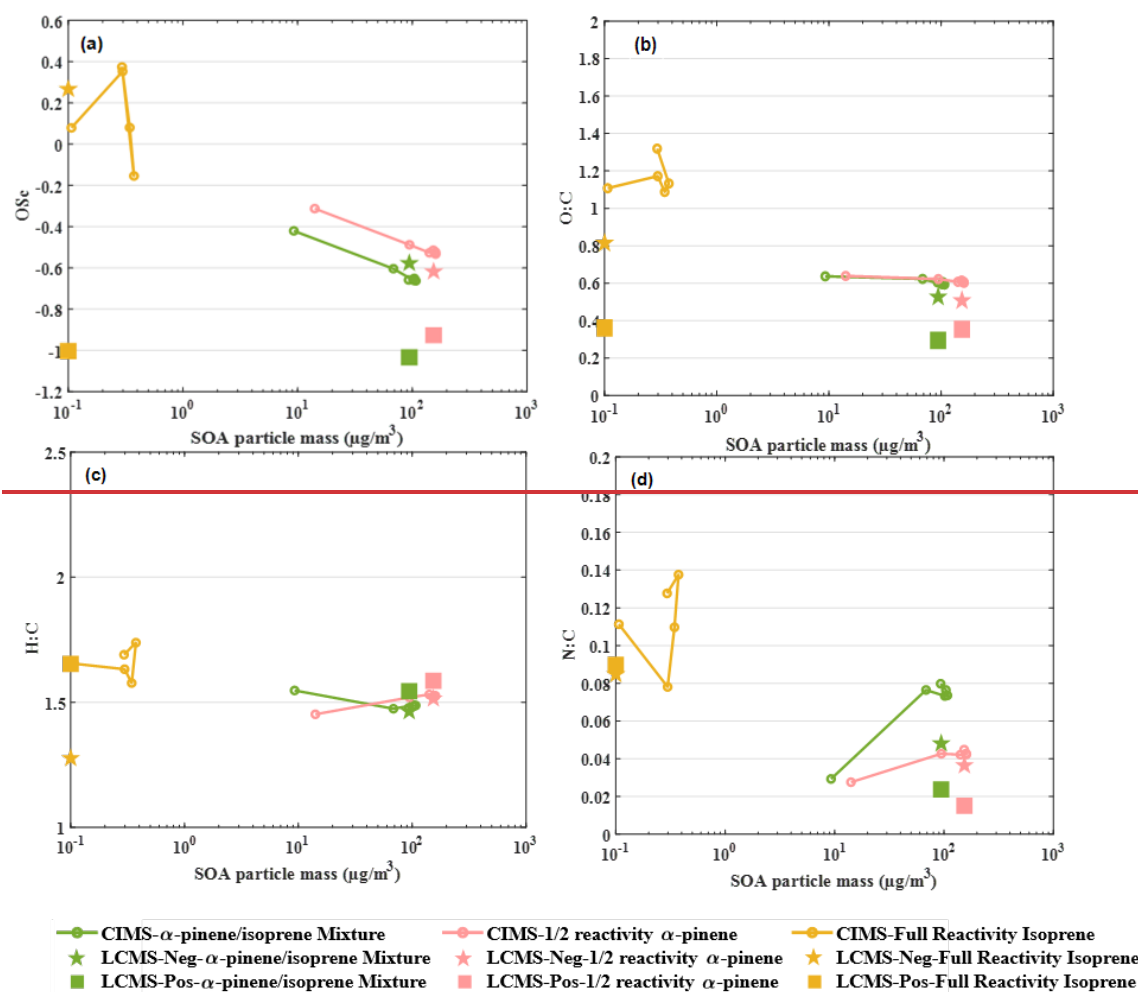


Figure 2: Evolution of SOA particle composition in terms of a) average carbon oxidation state ( $\overline{OSc}$ ), b) O/C, c) H/C and d) N/C atomic ratios as function of SOA mass concentration from FIGAERO-CIMS and UHPLC-HRMS measurements (-ve Ionization Mode (Neg) and +ve ionization mode (Pos)) in binary  $\alpha$ -pinene/isoprene mixture, 1/2 reactivity individual  $\alpha$ -pinene and full reactivity individual isoprene experiments.

### (b) *o*-cresol & isoprene binary system

Figure 3 shows the  $\overline{OSc}$ , O/C, H/C and N/C ratio of SOA particles derived from the FIGAERO-CIMS and UHPLC-HRMS in the binary *o*-cresol/isoprene system, individual 1/2 reactivity *o*-cresol and full reactivity isoprene experiments respectively. Again, owing to isoprene SOA has

minor mass contribution (less than chamber background concentration ( $<1 \mu\text{g m}^{-3}$ ) in the individual experiment, it might be expected that the  $\overline{OSc}$ , O/C, H/C and N/C ratio of SOA products from isoprene make a minor contribution in the binary *o*-cresol / isoprene system. Nevertheless, there are some significant differences between the individual VOC and mixture experiments.

The FIGAERO-CIMS  $\overline{OSc}$  in the individual *o*-cresol experiment and the mixture system both reduce with increasing particle mass, beyond  $3 \mu\text{g m}^{-3}$  (though the compounds in the particles are initially significantly more oxidised in the experiment on the mixture, so  $\overline{OSc}$  is initially higher, driven by a high O/C). The FIGAERO-CIMS  $\overline{OSc}$  in the mixture decreased from 0.38 at  $3 \mu\text{g m}^{-3}$  mass concentration to -0.21, while the  $\overline{OSc}$  in the individual *o*-cresol experiment showed a more modest decrease from 0.12 to -0.26 (Fig.3a). The FIGAERO-CIMS O/C and H/C in the mixture are higher than in the individual *o*-cresol experiment (Fig.3b and 3c). In particular the O/C behaved differently between the systems, in the mixture decreasing from 1.72 to 0.76 and in the individual *o*-cresol experiment, slightly increasing from an initial value of around -0.66 to a peak of 0.78 then falling towards the end of the experiment with increasing SOA mass concentration (Fig.3b). The H/C ratios simultaneously showed significantly decrease from 2.24 to 1.24 in the mixture system with a much smaller decrease from 1.32 to 1.09 in the individual *o*-cresol experiment (Fig.3c). It should be noted that this discrepancy in  $\overline{OSc}$  between the mixture system and sole *o*-cresol experiment is not seen in the HR-ToF-AMS data, which monotonically increased with SOA mass in the individual VOC and mixture system as shown in Fig. 6 (c), though of course this does not account for any nitrogen in the particles. Figure 3(d) shows that the FIGAERO-CIMS N/C ratio in both experiments increased with mass. This was more pronounced (from 0.02 to 0.12) in the mixture than in the individual *o*-cresol experiment (0.05 to 0.1).

$\overline{OSc}$  and O/C ratio from positive ionisation UHPLC-HRMS in the mixture and individual *o*-cresol experiments were of a comparable magnitude (roughly -0.5 and 0.45 respectively in both systems) though the H/C ratio is slightly higher in the mixture and N/C slightly lower (Fig.3e and 3d). From using negative ionisation measurements, Fig3e and 3d show that the mixture and individual *o*-cresol oxidation produces similar H/C and N/C ratios. Particles formed in the individual *o*-cresol experiment are marginally less oxidised ( $\overline{OSc} = -0.81$ ), than in the mixture system (-0.70), though overall the low degree of oxidation is driven by the high organic N content of the particles.

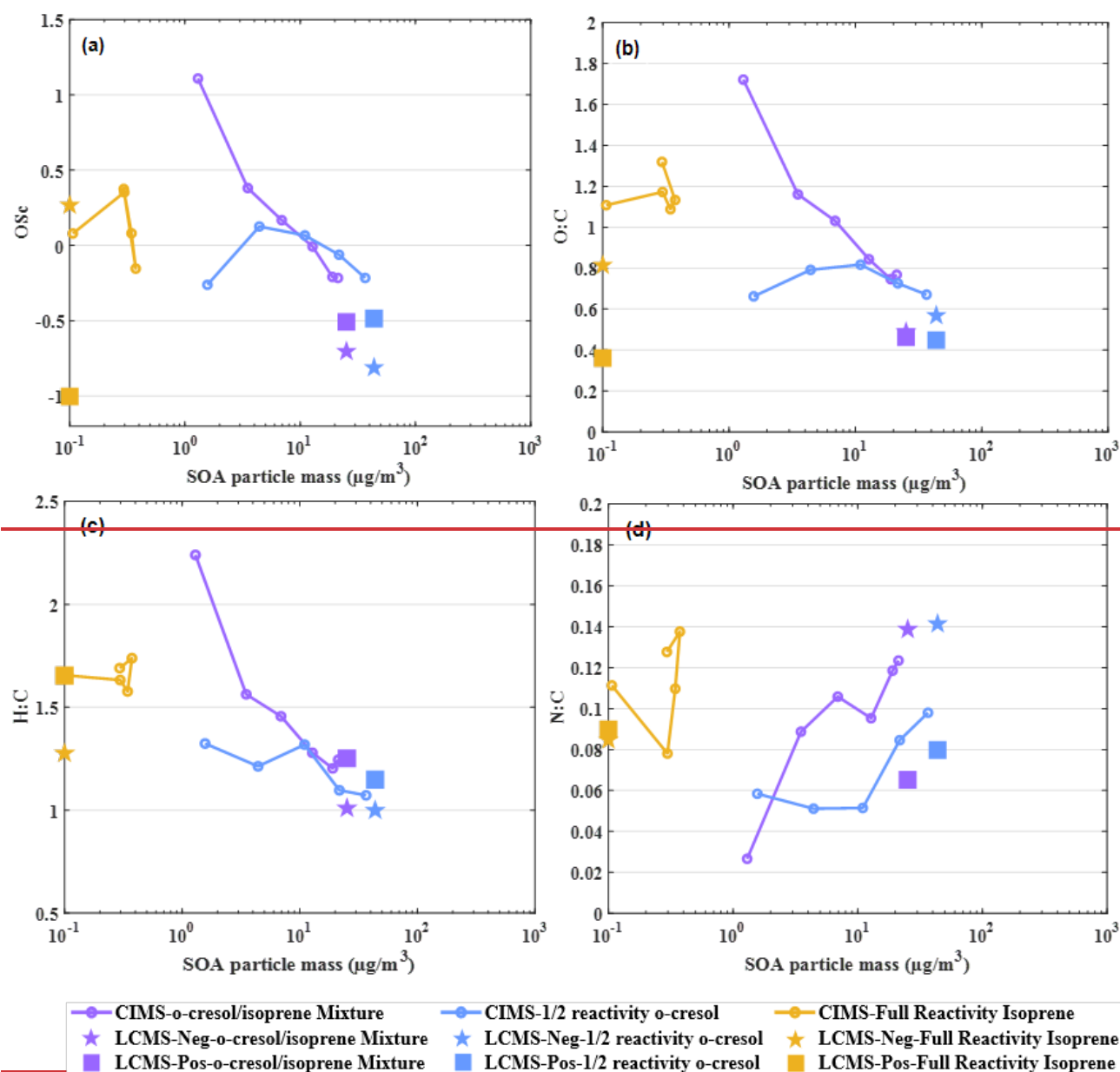


Figure 3: Evolution of SOA particle composition in terms of a) average carbon oxidation state ( $\overline{OSc}$ ), b) O/C, c) H/C and d) N/C atomic ratios as function of SOA mass concentration from FIGAERO-CIMS and UHPLC-HRMS measurements (-ve Ionization Mode (Neg) and +ve ionization mode (Pos)) in binary o-cresol /isoprene mixture, 1/2 reactivity individual o-cresol and full reactivity individual isoprene experiments.



### *(c) $\alpha$ -pinene & o-cresol Binary System*

Figure 4 shows the changes in  $\overline{OSc}$ , and atomic ratios (O/C, H/C and N/C) of SOA particles derived from FIGAERO-CIMS and UHPLC-HRMS in the binary  $\alpha$ -pinene / o-cresol mixture and the individual  $\frac{1}{2}$  reactivity precursor experiments. Panel a) shows that FIGAERO-CIMS average  $\overline{OSc}$  decreases with SOA mass concentration above  $3\mu\text{g}/\text{m}^3$  mass concentration in all experiments, though the  $\overline{OSc}$  is initially lower in the o-cresol experiment, driven by the low O/C.  $\overline{OSc}$  in the mixture system drop from 0.09 to -0.34 with increasing mass; a greater decrease than in the individual o-cresol ( $\overline{OSc} = 0.12$  to -0.26) and  $\alpha$ -pinene ( $\overline{OSc} = -0.31$  to -0.51) experiments. Overall, the gradient in the mixture experiment is similar to the  $\alpha$ -pinene experiment, but with an increase in the average degree of oxidation, though somewhat raised towards the o-cresol average  $\overline{OSc}$  by an increase in O/C. The O/C, H/C and N/C in the mixture system exhibit similar trends to the  $\alpha$ -pinene experiment (Fig.4b,4c and 4d) with absolute values in the mixture midway between the  $\alpha$ -pinene and o-cresol experiments (O/C falling from 0.82 to 0.63, N/C rising from 0.02 to 0.12, H/C modestly from 1.22 to 1.29).

The UHPLC-HRMS negative ionisation average  $\overline{OSc}$  and O/C ratio for the mixture were -0.63 and 0.52 respectively, comparable to those in the  $\alpha$ -pinene experiment. Positive ionisation mixture  $\overline{OSc}$  and O/C ratio values were both lower than the two single precursor values (Fig.4a and 4b). H/C and N/C ratios of the mixture in positive ionisation mode were similar to the o-cresol experiment (H/C=1.55, and N/C=0.55),

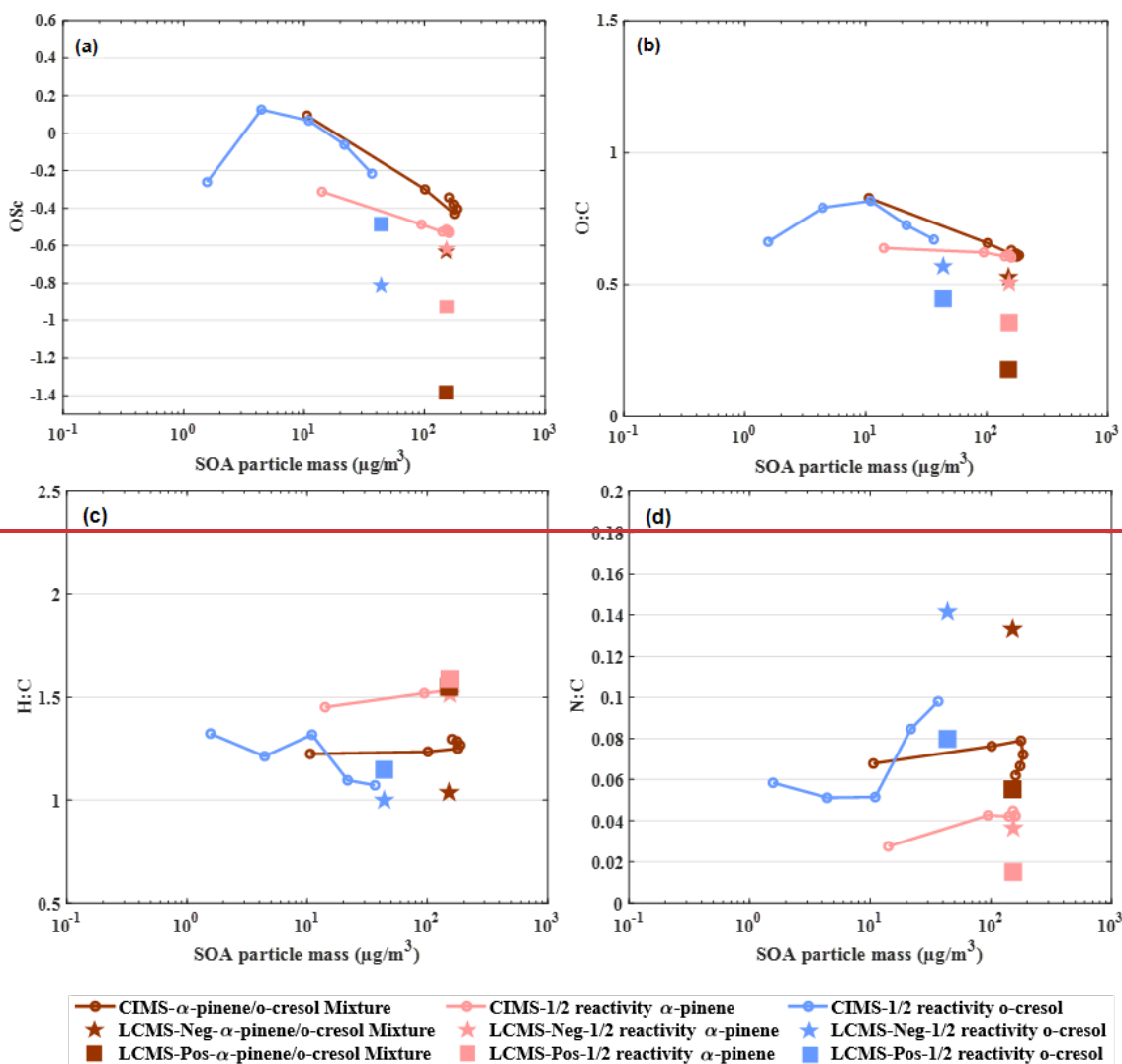


Figure 4: Evolution of SOA particle composition in terms of a) average carbon oxidation state  $\overline{OSc}$ , b) O/C, c) H/C and d) N/C atomic ratios as function of SOA mass concentration from FIGAERO-CIMS and UHPLC-HRMS measurements (–ve Ionization Mode (Neg) and +ve ionization mode (Pos)) in binary  $\alpha$ -pinene/*o*-cresol mixture,  $\frac{1}{2}$  reactivity individual  $\alpha$ -pinene and  $\frac{1}{2}$  reactivity individual *o*-cresol experiments.

#### (d) the ternary system

Figure 5 shows the change in average atomic ratios (O/C, H/C and N/C) and  $\overline{OSc}$  during SOA evolution in the ternary mixture system, along with  $\frac{1}{3}$  reactivity  $\alpha$ -pinene,  $\frac{1}{3}$  reactivity isoprene and  $\frac{1}{2}$  reactivity *o*-cresol experiments from FIGAERO-CIMS and UHPLC-HRMS measurements. The  $\frac{1}{3}$  reactivity *o*-cresol data were not available owing to instrumental failure. Fig.1e shows that the  $\overline{OSc}$  and atomic ratios are comparable between full reactivity and  $\frac{1}{2}$  reactivity *o*-cresol

experiments and it is plausible to expect similar molecular concentrations and hence aggregate properties in particles formed in the 1/2 and 1/3 reactivity individual *o*-cresol experiments.

Panel a) shows FIGAREO-CIMS average  $\overline{OSc}$  in the ternary mixture (decreasing in degree of oxidation from -0.16 to -0.35) is between that in the  $\alpha$ -pinene and *o*-cresol experiments, suggesting an influence from both precursors. Similarly, the mixture exhibits an average H/C ratio between the sole  $\alpha$ -pinene and *o*-cresol experiment, increasing from 1.30 to 1.47 (Fig.5e). The O/C and N/C ratios in the ternary mixture system increased with mass (O/C: 0.75 to 0.80, N/C: 0.07 to 0.09) and were higher than those in the  $\alpha$ -pinene and *o*-cresol experiments (Fig.5b and 5d). Approximately  $2\mu\text{g}/\text{m}^3$  of measurable products were generated in the 1/3 reactivity single isoprene experiment. The average  $\overline{OSc}$  decreased from 1 to -0.54, possibly owing to the significant increase in the H/C and N/C ratios (H/C: 1 to 1.9, N/C: 0.004 to 0.14) while the O/C ratios were comparable (O/C:  $\sim$ 0.9) for the 6 hours experiments in 1/3 reactivity single isoprene experiment.

The average  $\overline{OSc}$  in the  $\alpha$ -pinene/*o*-cresol binary mixture system (Brown line in Fig. 4a,  $\overline{OSc} \simeq 0.09$ ) are higher than the ternary mixture system in the early stage of experiment (Green line in Fig 5a,  $\overline{OSc} \simeq -0.16$ ), as obtained from the FIGAREO-CIMS though they have similar mass concentration ( $\sim 10\mu\text{g}/\text{m}^3$ ).

UHPLC-HRMS average  $\overline{OSc}$  and O/C ratios were similar to those in the sole  $\alpha$ -pinene experiments in both ionisation modes. However, the H/C and N/C ratio in the ternary mixture (H/C=1.52, N/C=0.03) was comparable to the  $\alpha$ -pinene experiment in positive ionisation modes. (Fig.5e and 5d), but closer to the *o*-cresol in negative. Also, the average  $\overline{OSc}$  and H/C ratios of ternary system were similar to those in the isoprene experiment in negative ionisation mode.

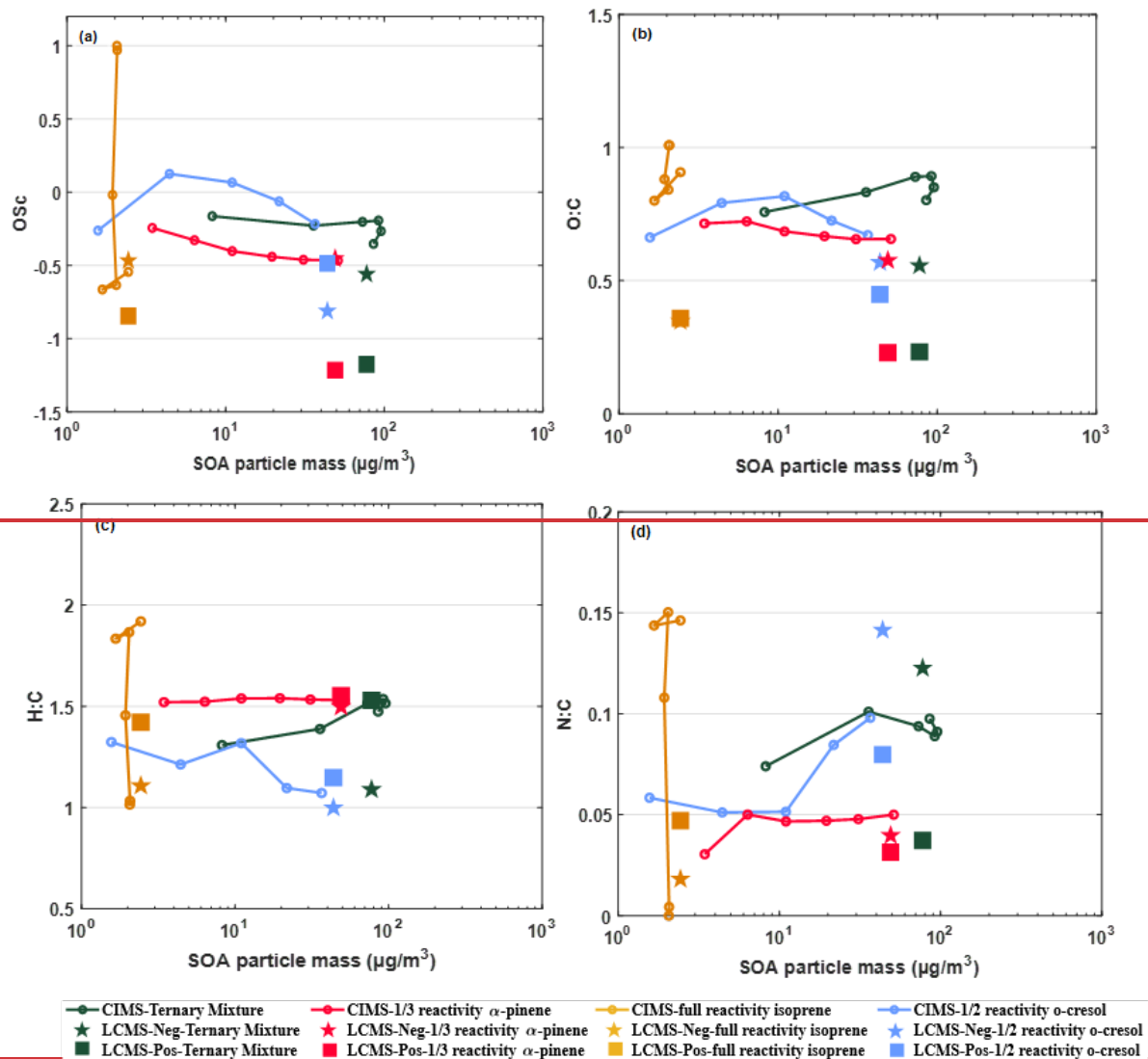


Figure 5: Evolution of SOA particle composition in terms of a) average carbon-oxidation state  $\overline{OSc}$ , b) O/C, c) H/C and d) N/C atomic ratios as function of SOA mass concentration from FIGAERO-CIMS and UHPLC-HRMS measurements (-ve Ionization Mode (Neg) and +ve ionization mode (Pos)) in ternary  $\alpha$ -pinene / o-cresol / isoprene mixture, 1/3 reactivity individual  $\alpha$ -pinene and 1/2 reactivity individual o-cresol experiments.

### 3.3. Average $\overline{OSc}$ Evolution in mixed precursor system (with $\overline{OS_N}$ correction)

#### 3.3.—Additional insight into $\overline{OSc}$ through inclusion of HR-ToF-AMS data

Figure 3 illustrated that the average  $\overline{OSc}$  evolution as a function of SOA mass concentration from mixture precursor system along with their reference single experiments, obtained from FIGAERO-CIMS and UHPLC-HRMS measurements. All values shown here include the  $\overline{OS_N}$  correction.

#### (a) $\alpha$ -pinene/Isoprene binary system

Figure 3a shows that the average  $\overline{OSc}$  in the half reactivity  $\alpha$ -pinene experiment exhibits a declining trend ( $-0.31$  to  $-0.51$ ) similar to that observed in the  $\alpha$ -pinene/isoprene binary mixture ( $\overline{OSc}$ :  $-0.42$  to  $-0.65$ ), based on FIGAERO-CIMS measurements. For comparison, we also include the single full reactivity isoprene experiment as a reference, noting that the single half reactivity isoprene experiments were not available. In the single isoprene experiment, SOA mass concentrations were negligible ( $<1 \mu\text{g m}^{-3}$ , close to chamber background), while the corresponding average  $\overline{OSc}$  remained between  $-0.2$  and  $0.4$ .

The UHPLC-HRMS results demonstrated comparable average  $\overline{OSc}$  in negative ionisation mode between the binary mixture and the single  $\alpha$ -pinene experiment (and aligns with the FIGAERO-CIMS endpoints at  $\overline{OSc} \approx -0.6$ ). In positive ionisation mode, however, the single full reactivity  $\alpha$ -pinene experiment shows a slightly higher  $\overline{OSc}$  than the mixture ( $\overline{OSc} \approx -0.92$ ) (Fig. 3a).

#### (b) *o*-Cresol/Isoprene binary system

From FIGAERO-CIMS measurement, both the binary *o*-Cresol/Isoprene and the single *o*-Cresol experiment display a decrease in average  $\overline{OSc}$  with increasing SOA mass beyond  $\sim 3 \mu\text{g m}^{-3}$  as shown in Figure 3b. In the binary mixture system, the average  $\overline{OSc}$  declines from  $0.38$  at  $3 \mu\text{g m}^{-3}$  to  $-0.21$  by the end of the experiment. For the single *o*-Cresol run, the average  $\overline{OSc}$  starts around  $-0.25$  during the initial low mass period ( $<3 \mu\text{g m}^{-3}$ , roughly the first hour), then decreases more modestly from  $0.12$  to  $-0.26$  as SOA mass increases (Fig. 3b). For reference, results from single isoprene experiments are also shown in Figure 3b. However, the SOA mass concentrations

were close to chamber background, so their average  $\overline{OSc}$  estimates should be interpreted with caution.

In the UHPLC-HRMS measurements, the positive ionisation mode has comparable average  $\overline{OSc}$  values for the binary mixture and single *o*-Cresol systems ( $\approx -0.50$ ). In contrast, the negative ionisation mode shows slightly higher average  $\overline{OSc}$  in the single *o*-Cresol experiment ( $\approx -0.55$ ) than in the binary mixture ( $\approx -0.71$ ) (Fig. 3b).

### **(c) *o*-Cresol/ $\alpha$ -pinene binary system**

Figure 3c shows that the FIGAERO-CIMS average  $\overline{OSc}$  decreases with SOA mass concentration above  $\sim 3 \mu\text{g m}^{-3}$  in the binary *o*-Cresol/ $\alpha$ -pinene system as well as in the single half reactivity *o*-Cresol and  $\alpha$ -pinene experiments. In the binary mixture system, the average  $\overline{OSc}$  declines from 0.09 to  $-0.34$ , a change comparable to that observed in the single half reactivity *o*-Cresol experiment (0.12 to  $-0.26$ ), but larger than in the single half reactivity  $\alpha$ -pinene experiment ( $-0.31$  to  $-0.51$ ).

In negative ionisation mode of UHPLC-HRMS measurement, the binary mixture has an average  $\overline{OSc}$  of  $-0.63$ , in reasonable agreement with the single half reactivity  $\alpha$ -pinene experiment. By contrast, in positive ionisation mode, the binary mixture produces a substantially lower average  $\overline{OSc}$  ( $\approx -1.38$ ) than either of the single precursors experiment, which were  $\approx -0.50$  for *o*-Cresol and  $\approx -0.92$  for  $\alpha$ -pinene.

### **(d) $\alpha$ -pinene/Isoprene/*o*-Cresol ternary system**

Figure 3d shows that the average  $\overline{OSc}$  exhibits a declining trend with increasing SOA mass in the ternary mixture system as well as in all single precursor experiments. In the ternary mixture system, the FIGAERO-CIMS average  $\overline{OSc}$  decreases from  $-0.16$  to  $-0.35$ , falling between the single third reactivity  $\alpha$ -pinene experiment ( $\overline{OSc}$  :  $-0.24$  to  $-0.26$ ) and the half reactivity *o*-Cresol experiment ( $\overline{OSc}$  : 0.10 to  $-0.21$ , excluding the first hour when SOA mass was very low). This suggests contributions from both precursors. It is noting that data for the third reactivity *o*-Cresol experiment were not available due to instrument failure. For isoprene, the single third reactivity experiment produced only  $\sim 2 \mu\text{g m}^{-3}$  of measurable SOA mass. In this case, the average  $\overline{OSc}$  estimated by FIGAERO-CIMS decreased sharply from  $\sim 1$  to  $-0.5$ .

The UHPLC-HRMS results show that in negative ionisation mode, the ternary mixture system has an average  $\overline{OSc}$  comparable to the single half reactivity *o*-Cresol experiment ( $\overline{OSc} \approx -0.55$ ), but slightly lower than the single third reactivity  $\alpha$ -pinene experiment ( $\overline{OSc} \approx -0.45$ ). By contrast, in positive ionisation mode the ternary mixture has an average  $\overline{OSc}$  similar to the single third reactivity  $\alpha$ -pinene experiment ( $\overline{OSc} \approx -1.2$ ) but much lower than the single half reactivity *o*-Cresol experiment ( $\overline{OSc} \approx -0.48$ ).

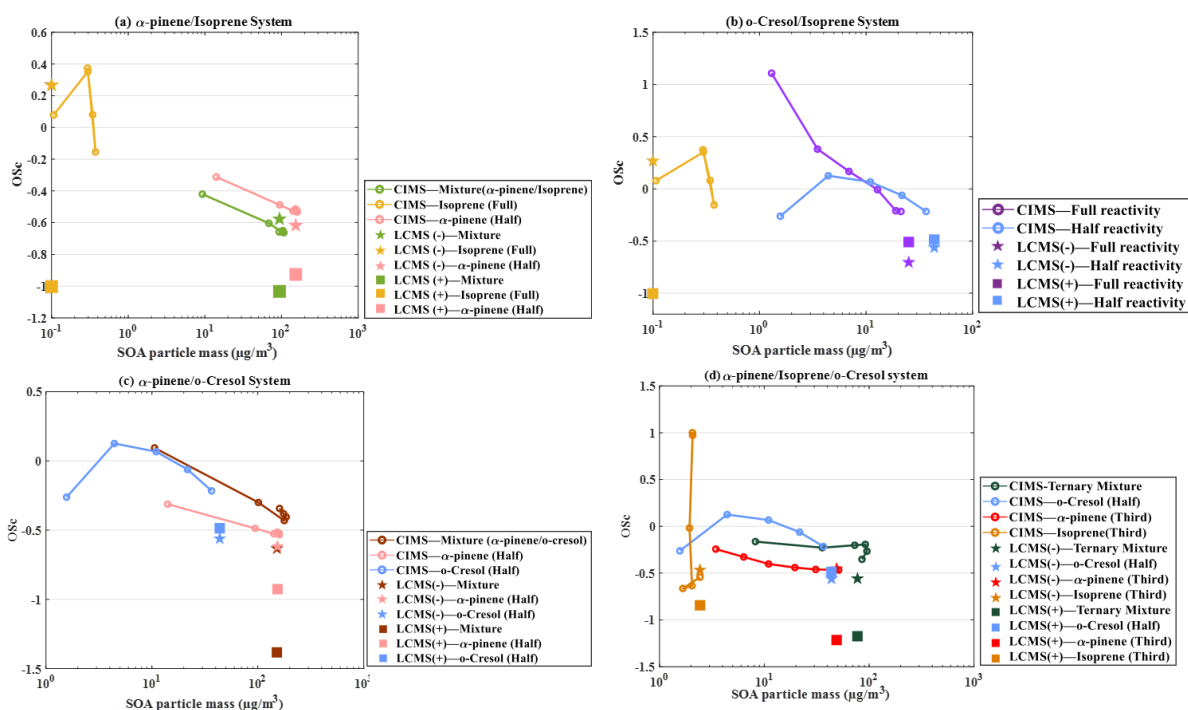


Figure 3. Evolution of the average  $\overline{OSc}$  (with  $\overline{OS_N}$  correction) as a function of SOA mass concentration for binary and ternary precursor systems, compared with the corresponding single precursor reference experiments. Results are shown from FIGAERO-CIMS (lines) and UHPLC-HRMS (symbols; negative ion mode = stars, positive ion mode = squares). Panels show (a)  $\alpha$ -pinene/ isoprene mixture, (b) *o*-Cresol /isoprene mixture, (c)  $\alpha$ -pinene/*o*-Cresol mixture, and (d) ternary  $\alpha$ -pinene + *o*-Cresol + isoprene system.

This section presents a comparison of the average carbon oxidation state of SOA particles detected by HR-ToF-AMS, FIGAERO-CIMS and UHPLC-HRMS techniques from mixed precursors systems and their corresponding single precursors experiments. Owing to the inability to reliably discern the N/C using the HR-ToF-AMS, the average carbon oxidation state presented in this section does not account for  $\overline{OS_N}$  calculated from all measurements. This allows for a comparison

of the compositional properties as measured by the three instruments, although these measurements are not directly comparable to those in section 3.2 that always has higher average  $\overline{OSc}$ .

Fig.6a suggests that the average  $\overline{OSc}$  of isoprene-derived compounds has only a modest influence on the carbon oxidation state in the binary  $\alpha$ -pinene/isoprene system when calculated from all MS measurements. HR-ToF-AMS derived  $\overline{OSc}$  in the mixture is comparable to the individual  $\alpha$ -pinene experiment at all particle mass concentrations and lower than the isoprene experiment (when only low particle mass was formed). Both systems exhibit an increase with SOA particle mass concentration up to  $\sim 10 \mu\text{gm}^{-3}$ , followed by reduction in the degree of oxidation as more mass was formed. The absolute values in the mixture ( $-0.33$  to  $-1.15$ ) were slightly lower than the individual  $\alpha$ -pinene values ( $-0.31$  to  $-0.99$ ). The FIGAERO-CIMS  $\overline{OSc}$  in the mixture were also close to the  $\alpha$ -pinene in trend and absolute values ( $-0.26$  to  $-0.27$ ) as were the UHPLC-HRMS average  $\overline{OSc}$  in both ionisation modes with the negative ionisation value close to those from the final HR-ToF-AMS measurement and slightly lower than from the FIGAERO-CIMS.

HR-ToF-AMS measurements in Fig.6b show  $\overline{OSc}$  of SOA formed in the *o*-cresol /  $\alpha$ -pinene binary mixture system falls between that of the SOA in the individual VOC experiments, indicating influence of oxidation products from both precursors.  $\overline{OSc}$  in the mixture initially increases (from  $-1.13$  to  $-0.30$ ) before falling to  $-0.5$  once the mass concentration had reached  $10.8 \mu\text{gm}^{-3}$ . A similar trend was seen in the  $\frac{1}{2}$  reactivity  $\alpha$ -pinene experiment at a lower  $\overline{OSc}$  value. The FIGAERO-CIMS  $\overline{OSc}$  in all systems was higher than the HR-ToF-AMS  $\overline{OSc}$  in the mixture ( $\overline{OSc} = 0.43$  to  $-0.03$ ) and  $\alpha$ -pinene experiments ( $\overline{OSc} = -0.17$  to  $-0.29$ ) following the same reducing trend, whilst the *o*-cresol  $\overline{OSc}$  increased to a plateau in both HR-ToF-AMS and FIGAERO-CIMS analyses. The UHPLC-HRMS  $\overline{OSc}$  of SOA in the mixture was  $-1.19$  in positive ionisation mode, lower than both the  $\alpha$ -pinene ( $\overline{OSc} = -0.87$ ), and *o*-cresol ( $\overline{OSc} = -0.25$ ) experiments. Negative mode  $\overline{OSc}$  in the mixture was  $0.02$ , which is  $0.11$  lower than for *o*-cresol and  $0.52$  higher than for  $\alpha$ -pinene (Fig.6b).

Fig.6c shows that the average  $\overline{OSc}$  of isoprene-derived compounds also only exert a modest influence on that of the binary *o*-cresol/isoprene binary mixture in measurements from all MS techniques. The HR-ToF-AMS measured  $\overline{OSc}$  in the mixture is comparable to that in the  $\frac{1}{2}$  reactivity *o*-cresol experiment, both increasing from  $-1.2$  to  $0.3$  at  $\sim 15 \mu\text{gm}^{-3}$  thereafter slightly



increasing in the mixture system (Fig.6e). The FIGAERO-CIMS  $\overline{OSc}$  in the mixture decreased from 1.2 to 0.2 with mass concentration increasing from  $1.3 \mu\text{g m}^{-3}$  to  $21.2 \mu\text{g m}^{-3}$ , whilst the single *o*-cresol  $\overline{OSc}$  increased from 0 to 0.27 across the same range of mass concentration, all values being higher than the HR-ToF-AMS  $\overline{OSc}$  until the highest mass concentrations. The  $\overline{OSc}$  in the mixture is comparable though slightly lower than that in the single *o*-cresol experiment after 6 hours in both ionisation mode of UHPLC-HRMS measurements.

Fig.6d shows that the average  $\overline{OSc}$  in the ternary mixture from HR-ToF-AMS increased marginally from -0.44 to a maximum of -0.22 with a mass concentration of  $11.84 \mu\text{g m}^{-3}$ , followed by a gradual decrease to -0.52. The single VOC  $\frac{1}{3}$  reactivity  $\alpha$ -pinene experiment showed a strong increase in  $\overline{OSc}$  from -2.51 to -0.66 and the  $\frac{1}{2}$  reactivity *o*-cresol experiment more gradually increasing from -1.2 to a plateau of 0.3 at  $15 \mu\text{g m}^{-3}$ . The average  $\overline{OSc}$  is around -1.7 in the  $\frac{1}{3}$  reactivity isoprene experiment with stable mass concentration of approximately  $1 \mu\text{g m}^{-3}$  for 6 hours experiment. The FIGAERO-CIMS average  $\overline{OSc}$  in for all experiments was consistently higher than the HR-ToF-AMS measurements as a function of SOA particle mass concentration. Moreover, the oxidation state in the ternary mixture experiment (0.13 to 0.2) was higher than that of the  $\alpha$ -pinene experiment but slightly lower than or comparable to the *o*-cresol experiment (0 to 0.2). Negative ionisation mode UHPLC-HRMS measurements showed the average ternary system  $\overline{OSc}$  to be similar to that in the *o*-cresol experiment, but positive mode was more comparable to that in the  $\alpha$ -pinene experiment. The average  $\overline{OSc}$  in the ternary mixture system as obtained from all instruments was dissimilar to that in the  $\frac{1}{3}$  reactivity isoprene experiment. Additionally, it is noteworthy that Fig.6 demonstrates good agreement between the negative ionisation mode results and the FIGAERO-CIMS measurements across all experiments.

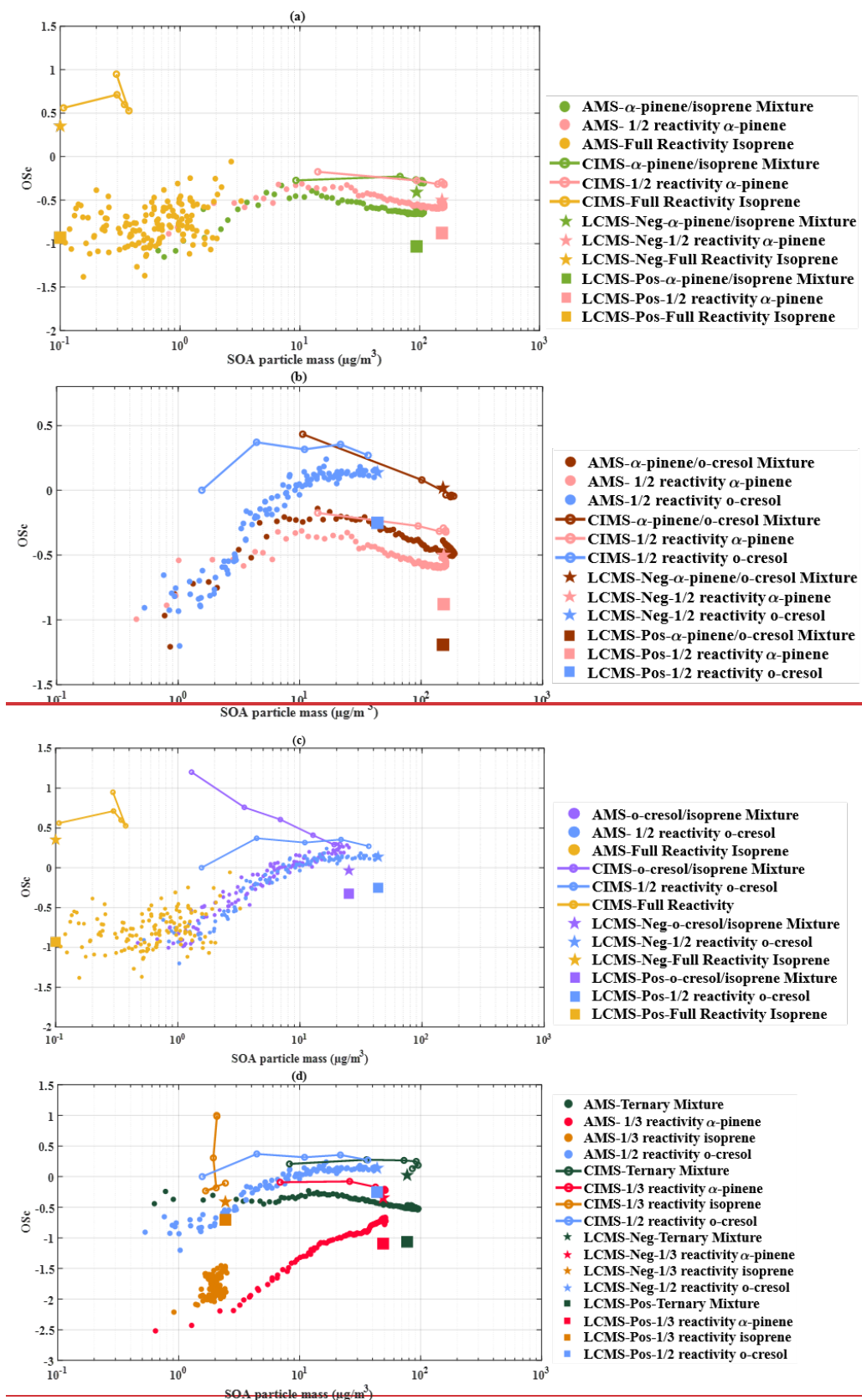


Figure 6:  $\overline{OSc}$  plotted as a function of SOA particle mass concentration in mixed precursor systems, a) binary  $\alpha$ -pinene /isoprene system; b) binary  $\alpha$ -pinene / *o*-cresol system; c) isoprene/*o*-cresol system, d) Ternary mixture precursor system from HR-ToF AMS, FIGAERO-CIMS and UHPLC-HRMS measurements (Negative Ionization Mode (Neg) and Positive ionization mode (Pos)).

## 4. Discussion

### 4.1. Average $\overline{OSc}$ Evolution with SOA Mass and Implication for Volatility and SOA Aging

#### 4.1. The application of multiple mass spectrometric techniques to the average oxidation state of carbon in SOA particles

The evolution of average  $\overline{OSc}$  that estimated accounting for the  $\overline{OS_N}$  term as a function of SOA mass could provide insight into the underlying chemical processes of SOA formation and aging. In the single  $\alpha$ -pinene and *o*-cresol experiments across all initial reactivities (Figs. 1),  $\overline{OSc}$  estimated from FIGAERO-CIMS measurements generally shows a declining trend as SOA mass increases. This behaviour suggested an increasing contribution from less oxidised material as particulate matters loading builds. It is possible that SOA growth is dominated by highly oxygenated, low-volatility products, likely formed via functionalisation of the precursor at the early stage. As SOA mass accumulates, the absorptive capacity of the particles increases, allowing semi-volatile, less oxidised compounds to partition, thereby driving down the bulk average  $\overline{OSc}$ . This interpretation is supported by the companion study of Voliotis et al. (2021), which reported pronounced fragmentation and a higher fraction of more-volatile product in the single  $\alpha$ -pinene system, that such species could contribute at later stages once sufficient mass has accumulated. Importantly, this relationship between average  $\overline{OSc}$  and SOA mass is consistent across different initial precursor concentrations. In the single  $\alpha$ -pinene experiments, all three reactivity levels (full, half, third) follow the same qualitative decline, showing that the observed behaviour is robust to starting conditions. For single *o*-Cresol experiments, the half reactivity experiment begins with lower average  $\overline{OSc}$  than the full reactivity experiment, but once the SOA mass reaches to comparable level, the two converge and decline together. This demonstrates that average

$\overline{OSc}$  evolution is primarily controlled by the partitioning balance during particle growth rather than the absolute precursor concentration.

The estimated average  $\overline{OSc}$  from UHPLC-HRMS (accounting for the  $\overline{OS_{N_1}}$  term) across the three  $\alpha$ -pinene experiments show small differences, but the  $\overline{OSc}$  in negative ionisation mode is consistently higher than in positive ionisation mode. A plausible explanation is that the negative ionisation mode preferentially detects deprotonated acids and highly oxygenated compounds (e.g. carboxylic acids) whereas the positive ionisation mode favours compounds with readily protonated functional groups, typically less acidic and less oxidised species. The negative ionisation mode  $\overline{OSc}$  also aligns closely with the FIGAERO-CIMS endpoint values, likely because both techniques are more sensitive to highly oxygenated, low-volatility species, and therefore capture a similar subset of the SOA composition. For the single *o*-Cresol system, the average  $\overline{OSc}$  in negative ionisation mode are comparable between the full and half reactivity experiments, that mainly contributed by nitro-aromatic molecules, which is dominate products in *o*-Cresol oxidation and to be sensitively detected in negative ionisation mode (Shao et al; 2022a). On the other hand, the positive ionisation mode average  $\overline{OSc}$  in half reactivity experiment is higher than full reactivity experiment, suggesting that the latter may contain a larger fraction of less-oxidised neutral species and oligomeric condensation products.

In this study, the average carbon oxidation state of SOA from different precursor systems was estimated from three mass spectrometry techniques measurements. The combination of online and offline mass spectrometric techniques to estimate the average  $\overline{OSc}$  of complex organic mixtures has not been widely adopted, particularly in the context of SOA components from the oxidation of mixed precursors in atmospheric simulation chamber studies. Each technique has its own strengths and limitations. The electrospray ionisation method used in the UHPLC-HRMS extraction can provide exact elemental ratios of individual compounds within organic mixtures using small sample volume. The FIGAERO-CIMS can provide molecular information for hundreds of particulate compounds in hourly timescale throughout a chamber experiment, with the low instrument backgrounds enabling detection limits in the picogram  $m^{-3}$  range for particle phase organic species (Lopez-Hilfiker et al., 2014). The average  $\overline{OSc}$  from FIGAERO-CIMS was determined using 6 measurements from the six thermal desorption cycles throughout each experiment, whilst the UHPLC-HRMS values were derived from analyses of filters collected at the end of each experiment. Both the UHPLC-HRMS and FIGAREO-CIMS techniques are

selective ionisation technique, with different response factor toward widely various components that may bias the average  $\overline{OSc}$  estimation. For instance, the negative ionisation mode in UHPLC-HRMS technique exhibits high sensitivity towards nitro-aromatic compounds (Shao et al., 2022a). Low volatility molecules may experience thermal decomposition in the FIGAERO-CIMS leading to fragmentation, influencing the average  $\overline{OSc}$  estimation (Du et al., 2021). The HR-ToF-AMS allows entire ensemble of SOA particles to be detected, fully fragmenting the flash vapourised particles by electron impact ionisation and measuring the elemental ratios in real time. This is the possible reason that we observed values of the FIGAERO-CIMS average  $\overline{OSc}$  were higher than the HR-ToF-AMS values and UHPLC-HRMS value in both single precursors' experiment (Fig.1b and 1d). The negative mode UHPLC-HRMS value in these two single precursors system is more comparable to HR-ToF-AMS value, but the positive mode UHPLC-HRMS values were lower. However, the accuracy of the retrieved elemental ratios is affected by uncertain empirical corrections in the analysis. Probably more importantly the average  $\overline{OSc}$  estimation obtained from our HR-ToF-AMS measurement cannot account for  $\overline{OS_{N^+}}$  given the limited resolution of the instrument calibrations. Farmer et al. (2010) reported the potential for overestimation of N and underestimation of O in ambient measurements by HR-ToF-AMS, highlighting the need for high-quality m/z calibrations and peak width/shape parameters when attempting to quantify nitrogen-containing compounds in HR-ToF-AMS spectra.

There are significant differences between carbon oxidation state (not accounting for  $\overline{OS_{N^+}}$ ) derived from the FIGAERO-CIMS measurements and those from HR-ToF-AMS under the same SOA mass concentration in all single experiments (Figs.1b and 1d) and mixed precursor systems (Fig.6 and Fig.1). The carbon oxidation state in FIGAERO-CIMS estimation is substantially higher than that in the HR-ToF-AMS measurement. The FIGAERO-CIMS used iodine as reagent ion, with an inherently higher sensitivity toward to the oxygenated organic compounds, biasing the measurements towards oxidized organic species (Lee et al., 2014). There is an additional possibility that thermal decomposition fragments may form from the larger organic molecules during the filter thermal desorption in the FIGAERO-CIMS that may potentially result in higher  $\overline{OSc}$  than their parent molecules. The average carbon oxidation state from FIGAERO-CIMS will depend on a subset of compounds biased towards higher oxidation state and consequently will be higher than that derived from HR-ToF-AMS and UHPLC-HRMS measurements. On the other

hand, the average  $\overline{OS_C}$  in the binary *o*-cresol/isoprene precursor system was high at the early stage of experiment (Fig. 6c), possibly indicating that the presence of isoprene influenced the early stages of the chemistry, though this requires further investigation. There is a substantial difference of average carbon oxidation state in the single VOC isoprene experiments (Fig. 6a and 6c), likely resulting from potential artefacts in the instruments and filter background since there was an insufficient amount of SOA particle mass produced in these experiments and the collected filter mass loading was low.

As stated, the average  $\overline{OS_C}$  comparisons with the HR-ToF-AMS discussed above do not account for the oxidation state of nitrogen ( $\overline{OS_N}$ ) and sulfur ( $\overline{OS_S}$ ) in their calculation. However, Organosulfate (CHONS and CHOS) and organonitrate (CHON and CHONS) have been reported in chamber experiments with  $NO_x$  and ammonium sulphate (Surratt et al., 2007; Surratt et al., 2008; Bruns et al., 2010; Fry et al., 2009). The heteroatom-containing groups will clearly impact on the derived  $\overline{OS_C}$  which should therefore be determined from  $2O/C - H/C - xN/C - yS/C$ , where x and y refer to the oxidation states of nitrogen ( $\overline{OS_N}$ ) and sulphur ( $\overline{OS_S}$ ) (Kroll et al., 2011). The uncertainty in HR-ToF-AMS  $\overline{OS_C}$  determination associated with S-containing groups is likely to be minimal since the S atom in weakly-bound species, such as organosulphates, tend not to be measured under thermal methods. This is not the case with nitrogen-containing compounds which may affect  $\overline{OS_C}$  determination, but unambiguous attribution of N is challenging at the limited resolution of the technique. Additionally, neutral losses can occur in the HR-ToF-AMS during thermal desorption, as some thermally labile or highly volatile compounds can desorb as neutral fragments (e.g.,  $CO_2$  or  $H_2O$ ). This can lead to an underestimation of certain oxygenated or heteroatom-containing species, biasing the measured elemental ratios (e.g., O:C and N:C) and adding uncertainty to the calculated average  $\overline{OS_C}$ .

The  $\overline{OS_N}$  of CHON compounds in FIGAERO-CIMS measurements clearly influenced the signal-weighted average  $\overline{OS_C}$ , consequently reducing the average  $\overline{OS_C}$ . The UHPLC-HRMS derived  $\overline{OS_C}$  is similarly influenced, particularly in *o*-cresol-containing systems in negative ionisation mode (owing to an enhanced sensitivity to specific CHON species likely formed through  $NO_2+OH$  radical reactions, dominated by nitro-aromatics as reported in Shao et al., 2022a) and the average  $\overline{OS_C}$  is significantly lower when accounting for  $\overline{OS_N}$ .

## 4.2. Influence of precursor mixture on average $\overline{OSc}$ during SOA formation

### 4.2. Comparison of SOA average Carbon Oxidation State at various precursor VOC concentration

While the metric  $\overline{OSc}$  in single volatile precursor systems has been considered, its application to SOA formed from mixtures of VOCs remains limited. Yet, in the real atmosphere, SOA almost always derives from multiple precursors undergoing simultaneous reactions. Examining how mixtures alter  $\overline{OSc}$  trends compared with single precursor experiment could offers novel insight into whether additional or modified chemical processes emerge when different VOCs simultaneous reacted. Beyond identifying these mechanistic differences, such comparisons provide useful constraints for future modelling efforts that aim to represent the chemical complexity of ambient SOA. To support this evaluation, this study presents the trend of average  $\overline{OSc}$  (account for  $\overline{OS_N}$  \*N/C correction term) driven from FIGAERO-CIMS and UHPLC-HRMS, shown as function of increasing SOA particle mass in binary and ternary mixture precursor mixture system, and compared against the corresponding single precursor reference experiments. Corresponding O:C, H:C, and N:C ratios for each mixture system are shown in the Supporting Information (Figs. S2-S5) to provide additional detail underlying the average  $\overline{OSc}$  evolution.

#### (a) $\alpha$ -pinene/Isoprene binary system

According to FIGAERO-CIMS measurement, both the  $\alpha$ -pinene/isoprene mixture system and the single half reactivity  $\alpha$ -pinene experiment show decreasing average  $\overline{OSc}$  with increasing SOA mass (Fig. 3a). However, the binary system is consistently offset to slightly lower  $\overline{OSc}$  at comparable mass loadings, likely reflecting suppression of highly oxygenated  $\alpha$ -pinene products by isoprene (via RO<sub>2</sub> competition and reduced HOM formation) and a larger relative contribution of less oxidised condensable molecules as the aerosol grows. Isoprene oxidation with OH radicals primarily produce semi-volatile C<sub>4</sub>–C<sub>5</sub> species with high volatility (e.g. hydroxycarbonyls), which could suppress  $\alpha$ -pinene SOA yields in mixed systems (Wennberg et al., 2018; Stroud et al., 2001; Carlton et al., 2009). An alternative interpretation is that these semi-volatile isoprene products partition onto the growing  $\alpha$ -pinene driven particle phase, lowering the average  $\overline{OSc}$  of the



1000 mixture. This interpretation is consistent with the findings of Voliotis et al. (2022a), where isoprene driven products accounted for ~3% of the total FIGAERO-CIMS signal in the binary system. Moreover, comparison across experiments indicates higher N/C ratios in the binary system than in the single half reactivity  $\alpha$ -pinene experiment (See Fig. S2(c)), suggesting that the presence of isoprene enhances the contribution of CHON species, which further drives down the average  $\overline{OSc}$  in the mixed system.

1005 The UHPLC-HRMS results fairly agree with these trends (Fig.3a). In negative ionisation mode, the mixed system has slightly higher average  $\overline{OSc}$  than the single half reactivity  $\alpha$ -pinene experiment, likely reflecting additional condensable acidic or highly oxygenated products from isoprene that are preferentially detected in negative ionisation mode. By contrast, in positive ionisation mode the binary system shows a slightly lower average  $\overline{OSc}$  than the single half reactivity  $\alpha$ -pinene experiment, which suggested the partitioning balance might shift toward less oxidised semi-volatile or oligomeric species when isoprene is present.

#### **(b) *o*-Cresol/Isoprene binary system**

1015 The binary *o*-Cresol/isoprene system shows an average  $\overline{OSc}$  evolution that can be described in two stages based on the FIGAERO-CIMS data. At the beginning of the experiment, when SOA mass was exceptionally low in both the binary and the single half reactivity *o*-Cresol system, the mixture exhibits a substantially higher average  $\overline{OSc}$  (Fig. 3b). This might suggest the formation of highly oxygenated accretion products when isoprene is present. Such HOM like species may arise from RO<sub>2</sub> cross reactions between isoprene and *o*-Cresol driven radicals, as well as from nitroaromatic compounds formed under NO<sub>x</sub> conditions. Although these species likely represent only a small fraction of the particle mass, their high oxygen content can disproportionately elevate the average  $\overline{OSc}$  at early stage of experiment.

1025 The average  $\overline{OSc}$  declines as SOA mass increases, that likely reflecting isoprene acts as an OH scavenger in the binary mixture system. This reduces the OH available for *o*-Cresol oxidation and suppresses the formation of highly oxidised *o*-Cresol products. Generally, *o*-Cresol RO<sub>2</sub> radicals generated via OH addition undergo autooxidation to form HOMs, but in the mixture these pathways potentially curtailed by competition with isoprene driven RO<sub>2</sub> and NO<sub>x</sub>. Instead of HOMs formation, the chemistry is likely diverted toward accretion or fragmentation channels, producing less oxidised products. This shift could reduce the contribution of highly oxygenated *o*-Cresol



products, explaining why the binary mixture system evolves toward lower average  $\overline{OSc}$  than the single half reactivity *o*-Cresol experiment at higher SOA mass.

In the UHPLC-HRMS measurements, the positive ionisation mode has comparable average  $\overline{OSc}$  values for both the single half reactivity *o*-Cresol and the binary *o*-Cresol/isoprene experiments (Fig. 3b), suggesting that both systems may generate a similar contribution of less acidic or neutral compounds. In contrast, the negative ionisation mode has higher average  $\overline{OSc}$  in the single half reactivity *o*-Cresol experiment compared with the binary mixture system. This likely reflects a relatively less contribution of CHON compounds in the single half reactivity *o*-Cresol experiment compared to the mixture system, as the negative ionisation mode is particularly sensitive to nitroaromatic species that dominate the CHON class. These nitrogen-containing oxygenated compounds could affect the  $\overline{OS}_N$  correction term, leading to lower average  $\overline{OSc}$  values when they are abundant. Previous work has shown that CHON compounds dominate *o*-Cresol SOA (>95% of the signal in both single and binary systems; Shao et al., 2022a), even though those results were obtained under full reactivity conditions. This observation still highlights the influence of CHON species in average  $\overline{OSc}$  estimation and reminds the importance of SOA chemical composition as well as by the compound classes to which each instrument is most sensitive.

### **(c) $\alpha$ -pinene/*o*-Cresol binary system**

The average  $\overline{OSc}$  in the  $\alpha$ -pinene/*o*-cresol binary system decreases as SOA mass grows that estimated from FIGAERO-CIMS measurement. At the early stage, the mixture exhibits average  $\overline{OSc}$  comparable to the single half reactivity *o*-Cresol experiment but consistently higher than the single half reactivity  $\alpha$ -pinene experiment at overlapping SOA mass (Fig.3c). One possible explanation is that FIGAERO-CIMS has high sensitivity to nitroaromatic products generated from *o*-Cresol oxidation (Voliotis et al. (2021), so the binary mixture system is weighted toward these highly oxygenated aromatic products. This sensitivity likely explains why the binary mixture system shows a similar magnitude of average  $\overline{OSc}$  to the single half reactivity *o*-Cresol experiment, despite  $\alpha$ -pinene being the higher SOA yield precursor. Toward the end of the experiment, the SOA mass of the binary mixture approaches that of the single half reactivity  $\alpha$ -pinene experiment, but its average  $\overline{OSc}$  remains higher, that might be attributed by the formation of additional multifunctional, low-volatility products via cross reactions between  $\alpha$ -pinene and *o*-Cresol driven  $RO_2$  radicals.

Interestingly, this behaviour is not consistent as the *o*-Cresol/isoprene binary system, where the mixture evolved to lower average  $\overline{OSc}$  than the single precursor experiment at the end of the experiment. The difference can be explained by isoprene driven RO<sub>2</sub> (highly volatile) suppresses the formation of highly oxygenated *o*-Cresol products, lowering the average  $\overline{OSc}$  as the SOA mass increased. whereas  $\alpha$ -pinene driven semi-volatile RO<sub>2</sub> favours the formation of multifunctional oxygenated accretion products that elevate the average  $\overline{OSc}$  of binary mixture system. Moreover,  $\alpha$ -pinene does not act as a strong OH scavenger compared with isoprene according to their reactivity (Dillon et al., 2017), so *o*-Cresol oxidation by OH might partly retained, and autoxidation of *o*-Cresol driven RO<sub>2</sub> may still proceed to form low volatility oxygenated dimers. The binary mixture system shows a slightly lower average  $\overline{OSc}$  than the single *o*-Cresol experiment in negative ionisation mode of UHPLC-HRMS measurement (Fig.3c). From the accompanying atomic ratios (See Fig.S4), this is driven by lower O:C and higher H:C ratio in the mixed precursor system, while N/C is comparable or smaller, which could explain that the difference is not due to a larger nitrogen containing compounds correction. In contrast, the average  $\overline{OSc}$  in the binary mixture is substantially lower than in either single precursor experiment in positive ionisation mode (Fig. 3c). This likely reflects a greater contribution of less acidic, lower O/C neutral species and oligomers produced through cross interactions in the binary mixture system compared to both single precursor experiment, which are preferentially detected in positive ionisation mode.

#### **(d) Ternary system**

The average  $\overline{OSc}$  in the ternary  $\alpha$ -pinene/*o*-Cresol/isoprene system decreases as SOA mass builds up (Fig. 3d) based on FIGAERO-CIMS measurement. Within the overlapping SOA mass range, the mixture sits between the single third reactivity  $\alpha$ -pinene and single half reactivity *o*-Cresol experiments, being higher than the  $\alpha$ -pinene experiment but lower than the *o*-Cresol experiment. This behaviour may suggest several competing chemical processes involve in the ternary mixture system rather than one dominate mechanism. For example, isoprene can act as an OH scavenger, slowing the multigenerational oxidation of  $\alpha$ -pinene and *o*-Cresol, and thereby suppressing the formation of highly oxygenated products. The presence of isoprene may also enhance the RO<sub>2</sub>+NO reaction, diverting chemistry toward organonitrates and fragmentation products, while limiting RO<sub>2</sub> + HO<sub>2</sub> pathways that typically drive functionalisation and higher average  $\overline{OSc}$ . Also, cross

interactions between *o*-Cresol driven RO<sub>2</sub> and  $\alpha$ -pinene or isoprene driven RO<sub>2</sub> could further suppress autoxidation of *o*-Cresol precursor, with consequences for both O/C and N/C atomic ratio. These effects together may explain why the ternary system evolves to intermediate  $\overline{OS_c}$  values, but the relative importance of each pathway remains unclear.

The UHPLC-HRMS negative ionisation mode reported the average  $\overline{OS_c}$  in the ternary mixture system is comparable to the single half-reactivity *o*-Cresol experiment, but slightly lower than the single third reactivity  $\alpha$ -pinene system (Fig. 3d). This suggests that nitroaromatic and other highly oxygenated CHON species, mainly characteristic of *o*-Cresol oxidation, remain an important contribution within the mixture system. In contrast, the positive ionisation mode indicates that the ternary mixture system aligns more closely with the single  $\alpha$ -pinene experiment. This points to a strong influence of neutral and oligomeric products in the ternary mixture system, likely including accretion products formed through cross-interactions between precursors.

The calculated carbon oxidation state of particles in the single precursor systems that generated significant mass ( $\alpha$ -pinene and *o*-cresol) with their initial concentration were compared. The initial “full” iso-reactive (accounting for their reactivity towards OH) concentration of the  $\alpha$ -pinene and *o*-cresol were 309 and 400 ppb. Experiments with half and third of these initial concentrations were also conducted to enable total initial iso-reactivity in the binary and ternary mixtures system. Further details can be found in Voliotis et al. (2022b).

FIGAERO-CIMS average  $\overline{OS_c}$  from the  $\alpha$ -pinene experiments accounting and not accounting for  $\overline{OS_x}$  is shown in Fig.1a and 1b, showing comparable values at all mass concentrations. In the HR-ToF-AMS initial 1/2 reactivity  $\alpha$ -pinene experiment showed a higher average  $\overline{OS_c}$  than full initial reactivity  $\alpha$ -pinene experiment, which was in turn higher than that from the 1/3 reactivity experiment (Fig.1b). It should be noted that the NO<sub>x</sub> concentration was reduced along with reduction of VOC initial concentration in half reactivity experiment in order to maintain a comparable VOC/NO<sub>x</sub> ratio across the system. This will influence the oxidant conditions, though it is unclear precisely why the oxidation state is so divergent at the lower particle mass concentrations within initial VOC concentration.

Unlike the  $\alpha$ -pinene precursor, the average  $\overline{OS_c}$  in the single precursor *o*-cresol experiment seems independent of initial precursors concentration in both HR-ToF-AMS and FIGAERO-CIMS measurement, whether or not  $\overline{OS_x}$  is considered (Fig.1b and 1d). The degrees of oxidation of

organic species appear comparable irrespective of initial *o*-cresol and NO<sub>x</sub> concentration. This might be due to the negligible reactivity of *o*-cresol towards O<sub>3</sub> (Atkinson, 2004). It should be noted that there is difficulty in reporting the O<sub>3</sub> direct measurement by UV absorption in the single precursor *o*-cresol experiment in this study owing to the UV absorption by *o*-cresol and its oxidation products. More details about the O<sub>3</sub> measurement by UV absorption was influenced by UV absorption by *o*-cresol was mentioned in the Voliotis et al. (2022b). However, this independence is less clear in the UHPLC-HRMS data, where a noticeably larger drop in average  $\overline{OSc}$  was observed in the 1/2 reactivity experiment when the  $\overline{OS_N}$  was included. This implies that CHON species, particularly highly oxidized, which may contribute more significantly to the overall composition under lower SOA mass loading.

Additionally, when the  $\overline{OS_N}$  is accounted for, the  $\overline{OSc}$  drop in the UHPLC-HRMS negative ionisation mode is larger than in FIGAERO-CIMS, especially in the 1/2 reactivity experiment ( $\delta \overline{OSc} = 0.95$  vs 0.48, respectively). This suggests that UHPLC-HRMS negative mode is more sensitive to CHON species that might highly be oxidized in low mass systems. In contrast, the full reactivity experiment shows a greater drop in FIGAERO-CIMS ( $\delta \overline{OSc} = 0.58$ ) than in UHPLC-HRMS ( $\delta \overline{OSc} = 0.70$ ), possibly reflecting greater sensitivity of FIGAERO-CIMS to semi-volatile nitrogen-containing species at higher SOA mass.

### 4.3. Average $\overline{OSc}$ Comparison across three Mass Spectrometry Techniques

#### 4.3. Comparison of SOA average Carbon Oxidation State accounting for $\overline{OS_N}$ in mixtures

Although  $\overline{OSc}$  is widely used as a metric to characterise SOA, its estimation depends strongly on the measurement technique. In this study, we shown a comparison across HR-ToF-AMS, FIAGERO-CIMS, and UHPLC-HRMS, to illustrate how instrumental properties impact the  $\overline{OSc}$  estimation of SOA particles. The combination of online and offline mass spectrometric techniques to estimate average  $\overline{OSc}$  has not been widely adopted, particularly in mixed precursor chamber studies.

From Fig.2, the FIGAERO-CIMS reported higher estimated average  $\overline{OSc}$  (not accounting for  $\overline{OS_N}$ ) compared to the UHPLC-HRMS and HR-ToF-AMS values in  $\alpha$ -pinene and *o*-Cresol experiments across all initial reactivities, that likely due to its strong sensitivity toward highly

oxygenated (Lee et al., 2014), low volatility compounds and the potential contribution of thermal decomposition fragments (Du et al., 2021). Moreover, the averaged  $\overline{OSc}$  in UHPLC-HRMS negative ionisation mode broadly agree with the FIGAERO-CIMS endpoint values, which might reflect their shared bias toward acidic and highly oxygenated compounds, whereas the positive ionisation mode more favour to detect the less oxidised neutral or oligomeric species leading to have lower average  $\overline{OSc}$ . The HR-ToF-AMS has average  $\overline{OSc}$  estimation generally lower than FIGAERO-CIMS but higher than positive ionisation mode of UHPLC-HRMS (Fig.2). For single  $\alpha$ -pinene experiments, HR-ToF-AMS has similar decline trend as the FIGAERO-CIMS in average  $\overline{OSc}$  in the full and half reactivity experiments but diverges in the third reactivity experiment, while for *o*-Cresol the HR-ToF-AMS reports an initial rise and then reach to a plateau. These discrepancies likely arise due to the HR-ToF-AMS being unable to unambiguously resolve nitrogen-containing species, so contributions from CHON and CHONS compounds are either missed or misattributed as CHO fragments. This limitation biases the elemental ratios, particularly lowering O/C and therefore depressing the calculated  $\overline{OSc}$ . Unlike the HR-ToF-AMS, the calculation of average  $\overline{OSc}$  in FIGAERO-CIMS and UHPLC-HRMS measurement still based on well-identified CHON compounds. This structural limitation suggested that HR-ToF-AMS estimated  $\overline{OSc}$  are not directly comparable to FIGAERO-CIMS/UHPLC-HRMS even when all are shown in “not accounting for  $\overline{OS_N}$ ” form. The issue is especially relevant for excessive aromatic and nitrate SOA, where organonitrate species (CHON, CHONS) are abundant in chamber experiments with NO<sub>x</sub> and ammonium sulphate (Surratt et al., 2007; Surratt et al., 2008; Bruns et al., 2010; Fry et al., 2009). In such cases, the true  $\overline{OSc}$  should be calculated as  $2O/C - H/C - xN/C - yS/C$  (Kroll et al., 2011). While the contribution of sulfur-containing groups is typically small, the nitrogen effect is substantial in average  $\overline{OSc}$  calculation. Moreover, neutral losses can occur in the HR-ToF-AMS during thermal desorption, as some thermally labile or highly volatile compounds can desorb as neutral fragments (e.g., CO<sub>2</sub> or H<sub>2</sub>O). This can also lead to an underestimation of certain oxygenated or heteroatom-containing species, biasing the measured elemental ratios (e.g., O:C and N:C) and adding uncertainty to the calculated average  $\overline{OSc}$ .

The average  $\overline{OSc}$  taking into account the  $\overline{OS_N}$ , H/C, O/C and N/C ratios in the mixtures (three binary and the ternary precursor system) and the corresponding single precursor systems were compared using the FIGAERO-CIMS and UHPLC-HRMS data.

#### **(a) $\alpha$ -pinene/isoprene binary mixture system**

The  $\frac{1}{2}$  reactivity single precursor  $\alpha$ -pinene experiment was used as reference experiment for binary mixtures containing  $\alpha$ -pinene, since it made a half contribution to the VOC reactivity. The trend of average  $\overline{OSc}$  in the  $\alpha$ -pinene/isoprene mixture system was comparable to that in the  $\frac{1}{2}$  reactivity  $\alpha$ -pinene experiments, suggesting that the dominant control by  $\alpha$ -pinene oxidation products (Fig.2a). This is unsurprising given the high established  $\alpha$ -pinene particle mass yield from OH oxidation in the presence of seed particles (Ahlberg et al., 2017; Eddingsaas et al., 2012; Henry et al., 2012). However, the magnitude of average  $\overline{OSc}$  in mixture system is slightly lower than in the single  $\alpha$ -pinene experiment, the influence of isoprene oxidation products on the average carbon oxidation state of total SOA. Isoprene is known to form C<sub>4</sub> and C<sub>5</sub> compounds with high volatility (e.g. methacrolein (C<sub>4</sub>) and C<sub>5</sub>-hydroxycarbonyls) on OH oxidation, with potential to suppress the particulate mass form from  $\alpha$ -pinene oxidation in the mixed system (Wennberg et al., 2018; Stroud et al., 2001; Carlton et al., 2009) (more information in section 4.5). Another possible interpretation is that the isoprene driven products (semi-volatile) partitioning in the mixture system due to high amount of adsorptive mass generated from the precursor  $\alpha$ -pinene, leading to lower the average  $\overline{OSc}$  in the binary  $\alpha$ -pinene/isoprene system compared to single  $\frac{1}{2}$  reactivity  $\alpha$ -pinene experiment. According to Voliotis et al. (2022a), the products resulting from isoprene contribute approximately 3% of the total signal observed in the measurement conducted with the FIGAERO-CIMS instrument in the binary  $\alpha$ -pinene/isoprene system. The difference in N/C ratios between  $\frac{1}{2}$  reactivity  $\alpha$ -pinene experiment and the binary mixture contributed to the difference in average  $\overline{OSc}$  and the H/C and O/C ratios were similar (Fig.2b and 2c), with N/C increasing with SOA particle mass in both systems. This suggests an increasing contribution of CHON compounds in both systems, with an increased contribution in the presence of isoprene.

#### **(b) *o*-cresol/Isoprene binary mixture system**

The FIGAERO-CIMS  $\overline{OSc}$  in the binary *o*-cresol/isoprene mixtures shared a broadly similar trend with the  $\frac{1}{2}$  reactivity single precursor *o*-cresol experiment. In addition, the binary mixture system has generally higher magnitude than the  $\frac{1}{2}$  reactivity single precursor *o*-cresol experiment apart from the measurement in the first half hour of the experiment. However,  $\overline{OSc}$  in the binary *o*-cresol/isoprene mixtures showed little similarity to the isoprene experiment  $\overline{OSc}$  (Fig.3a), suggesting a strong dependence on the *o*-cresol oxidation products. On the other hand, in the early stage of experiment (relatively low SOA mass), there is a high average  $\overline{OSc}$  in the binary system driven by the high O/C and low N/C compared to the  $\frac{1}{2}$  reactivity *o*-cresol experiment. This indicates an influence of isoprene at the early stages of the oxidation that could be a subject of further investigation. Whilst details of the mechanistic origins of this influence are unclear, Shao et al (2022a) report compounds uniquely found in this mixed system, but not in the oxidation of the individual precursors. Additionally, a clear divergence is observed between the N:C results in positive and negative ionisation modes obtained from UHPLC-HRMS (Fig.3d). This is likely due to the contribution of nitro-aromatic compounds generated from *o*-cresol oxidation, which are sensitively detected in negative ionisation mode.

#### (e) $\alpha$ -pinene/*o*-cresol binary mixture system

The average FIGAERO-CIMS  $\overline{OSc}$  in the binary  $\alpha$ -pinene/*o*-cresol system exhibited a similar trend to that in the  $\frac{1}{2}$  reactivity  $\alpha$ -pinene experiment at a higher magnitude, more comparable to that of the  $\frac{1}{2}$  reactivity *o*-cresol experiment (Fig.4a). This indicates that both  $\alpha$ -pinene and *o*-cresol contribute non-negligibly to the average  $\overline{OSc}$  in the mixture. According to the findings of Voliotis et al. (2021), the FIGAERO-CIMS demonstrated high sensitivity towards CHON products resulting from the oxidation of *o*-cresol. This high sensitivity might explain why the binary  $\alpha$ -pinene/*o*-cresol system shows a comparable magnitude of  $\overline{OSc}$  with the single  $\frac{1}{2}$  reactivity *o*-cresol system, despite  $\alpha$ -pinene being recognized as a precursor with higher SOA yield.

The O/C ratio contributed to the difference in  $\overline{OSc}$  (Brown line in Fig.4b,4c and 4d) more significantly than the H/C and N/C ratios. The O/C reduced with SOA particle mass, whilst H/C and N/C ratios remained constant, implying oxygen atoms loss (e.g.  $RO_2+R'O_2$  termination reactions) during the SOA production. Furthermore, the difference in  $\overline{OSc}$  could be influenced by the interaction between products of the individual precursors, with the unique compounds making a significant contribution. Voliotis et al. (2021) reported FIGAERO-CIMS measurement



of products uniquely found in this  $\alpha$ -pinene/*o*-cresol experiment, with the majority of these unique-to-mixture compounds having  $nC=5-10$  and  $nC>10$ . UHPLC-HRMS measurements reported in Shao et al., (2022a) also showed that high carbon number compounds contribute significantly in positive ionisation mode, likely cross-products from  $\alpha$ -pinene and *o*-cresol oxidation in either gas or particle phase.

#### (d) The ternary mixture

The FIGAERO-CIMS average  $\overline{OSC}$  in the ternary mixture does not follow a similar trend to any single VOC experiment (Fig.5a). The  $\overline{OSC}$  in this mixture was higher than in the  $\alpha$ -pinene, but lower than *o*-cresol experiment, and the average  $\overline{OSC}$  is likely not controlled by any single precursor. The trends in average atomic ratios (O/C, H/C and N/C) also have little similarity to those in the individual experiment (Fig.5b,5c and 5d), implying contributions from each of them. In the first half hour of the experiment, the average  $\overline{OSC}$  obtain from FIGAERO-CIMS in the ternary mixture was lower than in the  $\alpha$ -pinene/*o*-cresol binary mixture though both systems generated similar SOA particle mass concentration (Fig.5a). This may result from the early involvement of isoprene as an OH scavenger in the early stage of the experiment, leading to suppression of the low volatility and highly oxygenated products formed from  $\alpha$ -pinene and *o*-cresol oxidation. Oxidation in the ternary mixture may involve complex reactions that include interaction between radicals from the three individual precursors and alterations in the oxidation pathways of the individual precursors. The UHPLC-HRMS measurements in both ionisation modes further support the contention that each VOC contributes to the chemical composition in the ternary mixture, influencing the average carbon oxidation state, in addition to products uniquely found in the mixture (Fig.S1).



#### 4.4. Effect of $\overline{OS}_N$ accounting on average $\overline{OSc}$ estimation in single precursor system

##### 4.4. Comparison of average Carbon Oxidation State ignoring $\overline{OS}_N$ in the mixtures

This section evaluate the influence of the nitrogen correction term ( $\overline{OS}_N$ ) on the estimated  $\overline{OSc}$  in single  $\alpha$ -pinene and *o*-Cresol experiments using FIGAERO-CIMS and UHPLC-HRMS measurements.

As noted earlier, accounting for  $\overline{OS}_N$  can have non-negligible effect on the estimation of average  $\overline{OSc}$  of bulk SOA. Table 2 that shown below summarised the average  $\overline{OSc}$  of single  $\alpha$ -pinene and *o*-Cresol experiments across all reactivities estimated from FIGAERO-CIMS and UHPLC-HRMS measurement. This reported that ignoring  $\overline{OS}_N$  term generally biases the estimation of average  $\overline{OSc}$  upward, leading to consistently higher average  $\overline{OSc}$  values across both instrument (All  $\Delta \overline{OSc} < 0$ ).

In the single  $\alpha$ -pinene experiments, the downward adjustment associated with including the nitrogen correction term ( $\overline{OS}_N \cdot \text{N/C}$ ) is fairly consistent across FIGAERO-CIMS and UHPLC-HRMS measurement ( $\Delta \overline{OSc} \approx -0.05$  to  $-0.2$ ), which might suggest relatively small contribution of N-containing products at the endpoints. By contrast, the corrections are much larger in the single *o*-Cresol experiments, particularly in the UHPLC-HRMS negative ionisation mode ( $\Delta \overline{OSc} \approx -0.43$  to  $-0.70$ ) and FIGAERO-CIMS measurement ( $\Delta \overline{OSc} \approx \sim 0.5$ ), with moderate values in UHPLC-HRMS positive ionisation mode ( $\Delta \overline{OSc} \approx -0.23$  to  $-0.29$ ). The larger adjustment in *o*-Cresol experiments likely arises from the fact that its oxidation is dominated by nitroaromatic oxygenated compounds. These nitrogen containing species are particularly well captured in the negative ion mode of UHPLC-HRMS (and also by CIMS), and because of their abundance, they contribute strong influence on the  $\overline{OS}_N \cdot \text{N/C}$  correction term. As a result, their dominance drives a pronounced reduction in the estimated average  $\overline{OSc}$ .

It is important to note that, for FIGAERO-CIMS and UHPLC-HRMS, including or excluding the  $\overline{OS}_N$  correction term in the average  $\overline{OSc}$  calculation is a deliberate choice, and its impact depends

strongly on the identified chemical composition of the SOA. By contrast, the HR-ToF-AMS cannot resolve nitrogen-containing products, which leads to systematic misattribution of CHON species as CHO fragments. This structural limitation, as discussed in Section 4.3, highlights the need for caution when interpreting AMS-derived  $\overline{OSc}$  values, as the inability to account for  $\overline{OS_N}$  can bias comparisons with FIGAERO-CIMS and UHPLC-HRMS measurements.

~~This section assesses the influence of individual precursors on  $\overline{OSc}$  in mixtures without accounting for  $\overline{OS_N}$  using HR-ToF-AMS, FIGAERO-CIMS and UHPLC-HRMS measurements.~~

~~In binary isoprene-containing mixtures, the  $\overline{OSc}$  from all three instruments showed no clear similarity to the full reactivity isoprene experiment (Fig.6a and 6c), in agreement with the values accounting for  $\overline{OS_N}$  (Fig. 2a and 3a).  $\alpha$ -pinene and *o*-cresol products controlled  $\overline{OSc}$  in their respective mixtures with isoprene. The ternary mixture again displayed a non-additive behaviour, with average  $\overline{OSc}$  values falling between those of  $\alpha$ -pinene and *o*-cresol, similar to the  $\alpha$ -pinene/*o*-cresol binary mixture (Fig.6d). The trend in HR-ToF-AMS  $\overline{OSc}$  in the  $\alpha$ -pinene/*o*-cresol binary mixture most closely followed that of the  $\alpha$ -pinene experiment but increased slightly towards that of *o*-cresol (Fig.6b). Both *o*-cresol and  $\alpha$ -pinene products likely contributed to the average  $\overline{OSc}$  in their binary mixture, but possibly more from  $\alpha$ -pinene. The FIGAERO-CIMS  $\overline{OSc}$  presents a contrary picture, with the trend following that of  $\alpha$ -pinene, but absolute value closer to that of *o*-cresol.~~

Table 2: Average  $\overline{OSc}$  for single  $\alpha$ -pinene and o-Cresol experiments across all reactivities, estimated from FIGAERO-CIMS (hereafter CIMS), and UHPLC-HRMS (hereafter, LCMS) measurement. For FIGAERO-CIMS, values correspond to the endpoint of each experiment, while UHPLC-HRMS values are based on filter extracts collected at the experiment endpoint.  $\overline{OSc}$  was estimated both accounting or not accounting the term of  $\overline{OS_N}$ , and the difference  $\Delta \overline{OSc} = \overline{OSc}$  (accounting  $\overline{OS_N}$ ) -  $\overline{OSc}$  (not accounting  $\overline{OS_N}$ ).

<u>Precursor</u>	<u>Initial Conditions (Reactivity)</u>	<u>Instrument</u>	<u><math>\overline{OSc}</math> (Accounting <math>\overline{OS_N}</math>)</u>	<u><math>\overline{OSc}</math> (Not accounting <math>\overline{OS_N}</math>)</u>	<u><math>\Delta \overline{OSc}</math></u>
<u><math>\alpha</math>-pinene</u>	<u>Full</u>	<u>CIMS</u>	<u>-0.57</u>	<u>-0.40</u>	<u>-0.17</u>
		<u>LCMS (-ve mode)</u>	<u>-0.58</u>	<u>-0.44</u>	<u>-0.14</u>
		<u>LCMS (+ve mode)</u>	<u>-0.99</u>	<u>-0.91</u>	<u>-0.08</u>
	<u>Half</u>	<u>CIMS</u>	<u>-0.52</u>	<u>-0.31</u>	<u>-0.21</u>
		<u>LCMS (-ve mode)</u>	<u>-0.61</u>	<u>-0.5</u>	<u>-0.11</u>
		<u>LCMS (+ve mode)</u>	<u>-0.92</u>	<u>-0.87</u>	<u>-0.05</u>
	<u>Third</u>	<u>CIMS</u>	<u>-0.46</u>	<u>-0.22</u>	<u>-0.24</u>
		<u>LCMS (-ve mode)</u>	<u>-0.45</u>	<u>-0.34</u>	<u>-0.11</u>
		<u>LCMS (+ve mode)</u>	<u>-1.21</u>	<u>-1.09</u>	<u>-0.12</u>
<u>o-Cresol</u>	<u>Full</u>	<u>CIMS</u>	<u>-0.37</u>	<u>0.21</u>	<u>-0.58</u>
		<u>LCMS (-ve mode)</u>	<u>-0.55</u>	<u>0.15</u>	<u>-0.7</u>
		<u>LCMS (+ve mode)</u>	<u>-0.66</u>	<u>-0.37</u>	<u>-0.29</u>
	<u>Half</u>	<u>CIMS</u>	<u>-0.21</u>	<u>0.27</u>	<u>-0.48</u>
		<u>LCMS (-ve mode)</u>	<u>-0.56</u>	<u>-0.13</u>	<u>-0.43</u>
		<u>LCMS (+ve mode)</u>	<u>-0.48</u>	<u>-0.25</u>	<u>-0.23</u>

#### 4.5.— Drivers for carbon oxidation state behaviour

Knowing the oxidation pathway of precursors provides a description of the chemical behaviour of the mixed systems controlling average carbon oxidation state during SOA formation and evolution. The oxidant regime (OH and O<sub>3</sub>) during the experiments can differ between the mixture and individual precursor experiments despite our best attempts to maintain similar conditions through initial “iso-reactivity” as explained in Voliotis et al. (2022b). The ozone production and hence OH profile may not be the same in the mixture as in the individual precursor experiments and the reactivity towards the available oxidants will not remain equal. This, in turn, will lead to changes in the timescale of product formation from each of the reactants. Both α-pinene and isoprene are readily oxidized by both OH and O<sub>3</sub>, while the *o*-cresol is unreactive towards O<sub>3</sub> owing to its stable aromatic ring and lack of double bond. This section discusses the drivers causing different carbon oxidation state between single and mixture precursors system with reference to the various classes of potential reactions (e.g. functionalization-oligomerization, and fragmentation).

The FIGAERO-CIMS results suggest that the carbon oxidation state profile accounting for  $\overline{OS_N}$  is higher in single α-pinene experiment compared to its mixture with isoprene (Fig. 2a), but carbon oxidation state profile is similar if  $\overline{OS_N}$  is not considered (Fig. 6a). Fig. 6a also shows that the HR-ToF-AMS average  $\overline{OSC}$  in the mixture is lower than in the individual α-pinene experiment. Voliotis et al. (2022a) reported that the binary α-pinene/isoprene system exhibits a lower SOA mass yield compared to the sole α-pinene experiment. While this may initially suggest a suppression in the formation of low volatility α-pinene oxidation products due to competition for oxidants, Voliotis et al. (2022a) showed that the volatility distribution of the SOA from the α-pinene/isoprene mixture was comparable to that from the α-pinene-only experiment. This might be attributed to the formation of new products in the mixture, which had similar volatility characteristics to those from the α-pinene SOA. However, the chemical composition was distinctly altered, with some α-pinene products being suppressed and unique compounds forming in the presence of isoprene. These changes in chemical composition, rather than volatility, may help explain the observed decrease in average carbon oxidation state and SOA mass in the mixed system.

In the isoprene / *o*-cresol system, the average  $\overline{OSC}$  derived from both online and offline mass spectrometry were comparable to that obtain in the individual *o*-cresol experiment, apart from the early state of FIGAERO-CIMS measurement, as discussed in section 4.3 (b) (Fig. 3a and 6c). The wall-loss-corrected particle mass in the mixture was lower than in the *o*-cresol experiment (as

reported by Voliotis et al. (2022b)). This may be a result of the isoprene scavenging the available OH oxidants in the binary precursor system or reacting with O<sub>3</sub> which would otherwise have been available to form OH, both effects leading to reducing the SOA particle mass concentration from *o*-cresol oxidation (Voliotis et al., 2022b). A similar average  $\overline{OSc}$  was observed between the two systems, which is reasonable since the chemical composition of SOA formed from binary isoprene / *o*-cresol system show strong resemblance the single *o*-cresol experiment, with the dominance of CHON compounds with seven carbon atoms (C<sub>7</sub>H<sub>7</sub>NO<sub>3</sub>, and C<sub>7</sub>H<sub>7</sub>NO<sub>4</sub> compounds) as identified by FIGAREO-CIMS and UHPLC-HRMS (Shao et al., 2022a; Voliotis et al., 2022a). Initially, it was hypothesized that isoprene might act as an OH scavenger, thereby limiting *o*-cresol oxidation, as seen in other systems such as  $\alpha$ -pinene/isoprene mixtures. However, the similar average  $\overline{OSc}$  values between the single precursor *o*-cresol and binary *o*-cresol/isoprene systems suggest that this may not be play a dominant role in this case. A plausible explanation is the presence of elevated ozone in the binary system, which will lead both to increased production of OH via O<sub>3</sub> photolysis and to increased consumption of isoprene and possibly *o*-cresol oxidation products (see Fig. S2 in [Voliotis et al., 2022b]). Additionally, unique to mixture products are formed in the binary *o*-cresol/isoprene system, which may also contribute to the average  $\overline{OSc}$  in the binary system (Voliotis et al., 2022a, Shao et al., 2022a). These explanations remain speculative and highlight the need for mechanistic studies investigating the SOA formation in this particular binary system.

In the binary  $\alpha$ -pinene / *o*-cresol system, the FIGAERO-CIMS and HR-ToF-AMS carbon oxidation states have a similar trend to the individual  $\alpha$ -pinene experiment though the absolute value in the mixture was between the *o*-cresol and  $\alpha$ -pinene values whether accounting for  $\overline{OS_N}$  or not in all instruments (Fig.4a and Fig.6b). Mixing *o*-cresol with  $\alpha$ -pinene will increase the degree of oxidation at any given mass loading and enhancing the average  $\overline{OSc}$  compared to single  $\alpha$ -pinene experiment. These products may be partially attributed to formation of gaseous cross-product formation from  $\alpha$ -pinene and *o*-cresol followed by condensation in the mixed system. More molecular information about the cross-products formation and potential mechanistic differences between the mixtures and individual precursor experiment leading to compounds uniquely found in the binary  $\alpha$ -pinene/*o*-cresol mixture have been reported by Voliotis et al. (2021) and (Shao et al., 2022a)

In the ternary mixture, the absolute magnitude of the average carbon oxidation state was between the individual *o*-cresol and  $\alpha$ -pinene experiments. The average  $\overline{OSc}$  of the ternary system is similar to the binary *o*-cresol/ $\alpha$ -pinene system, but the trend with SOA particle mass concentration was not the same as in any individual precursor experiment (Fig.5, and Fig.6d). This may be attributed to the more complex chemistry in ternary system. Both *o*-cresol and  $\alpha$ -pinene derived products contributed to the chemical composition as Shao, et al, (2022a) reported, with negligible contribution of isoprene driven products. This would lead to the average  $\overline{OSc}$  in ternary mixture being higher than that in the individual  $\alpha$ -pinene experiment with more oxygenated compounds being *o*-cresol oxidation products. Meanwhile, the significant higher SOA particle mass in ternary mixture compared to any single precursor experiment (single  $1/3$  reactivity  $\alpha$ -pinene, single  $1/2$  reactivity *o*-cresol and  $1/3$  reactivity isoprene) might partially attributed to the formation of gaseous cross products that subsequently condense. This is consistent with both Voliotis et al. (2021) and Shao et al. (2022a) who reported that compounds uniquely found in the mixture made non-negligible contribution in ternary system. This cross-interaction between molecules might include  $RO_2+R'O_2$  termination reactions (oxygen atoms loss process as we mentioned in 4.3) leading to generate an increase in less oxygenated organic species, reducing average  $\overline{OSc}$  during particulate matter formation.

## 5. Conclusion

### 5. Summary

This study reframes the interpretation of SOA chemistry by using average  $\overline{OSc}$  as a diagnostic tool to explore the evolution of SOA from both single and mixed precursor systems. Rather than focusing on detailed product identification, which has been addressed in our previous work, we emphasise how  $\overline{OSc}$  trends provide broader insights into volatility, aging pathways, and precursor interactions.

We reported that average  $\overline{OSc}$  generally declines as SOA mass increases in all mixed precursor systems, consistent with an increasing role of semi-volatile and less oxidised species at higher loadings from FIGAERO-CIMS measurement (accounting for  $\overline{OS_N}$  correction). This behaviour

seems highlights the role of  $\overline{OSc}$  as a proxy for functionalisation versus fragmentation pathways and SOA volatility.

Another finding of this study is that inclusion of the  $\overline{OS_N}$  correction substantially reduces average  $\overline{OSc}$  estimates, particularly in *o*-Cresol experiment, which is dominate with CHON products, suggested that chemical composition and calculation choices directly influence the mechanism interpretation about SOA oxidation.

Comparisons of average  $\overline{OSc}$  across FIGAERO-CIMS, UHPLC-HRMS, and HR-ToF-AMS further reveal systematic discrepancies in this study. Both the FIGAERO-CIMS and UHPLC-HRMS could identify the molecule composition, including the CHON species, whereas the HR-ToF-AMS cannot resolve nitrogen-containing species. This limitation likely results in CHON signals being misattributed as CHO, leading to introduce systematically bias to O/C and thereby the calculating  $\overline{OSc}$ .

Beyond instrument specific biases, the mixture precursors experiments highlight that the precursor interactions, such as OH scavenging by isoprene, NO<sub>x</sub> driven RO<sub>2</sub> competition, and cross interaction between RO<sub>2</sub> from different precursor could change the balance of functionalisation and fragmentation, producing average  $\overline{OSc}$  trajectories distinct from those of single VOCs.

~~The average carbon oxidation state and atomic ratios (H/C, O/C and N/C) of SOA formed from photooxidation of  $\alpha$  pinene, isoprene, *o*-cresol and their binary and ternary mixtures in the presence of NO<sub>x</sub> and ammonium sulphate seed particles was determined by HR-ToF-AMS, FIGAERO-CIMS and UHPLC-HRMS. Factors affecting the average  $\overline{OSc}$  during SOA evolution in mixed precursor systems were interrogated by combining these online and offline mass spectrometer measurements.~~

~~The average  $\overline{OSc}$  obtained from FIGAERO-CIMS and UHPLC-HRMS were calculated both accounting for, and not accounting for  $\overline{OS_N}$ .  $\overline{OS_N}$  was inaccessible to the HR-ToF-AMS due to its limited resolution and hence average  $\overline{OSc}$  did not account for  $\overline{OS_N}$ . Average  $\overline{OSc}$  not considering  $\overline{OS_N}$  showed substantial difference between the FIGAERO-CIMS, HR-ToF-AMS and UHPLC-HRMS measurements, with the FIGAERO-CIMS and UHPLC-HRMS only measuring a subset of compounds. The FIGAERO-CIMS has higher sensitivity toward more oxygenate compounds, and UHPLC-HRMS has a particularly high sensitivity to aromatic nitro-compounds in negative ionisation mode.~~

The average carbon oxidation obtained from FIGAERO-CIMS and UHPLC-HRMS appears unaffected by the initial precursor concentration in the single precursor  $\alpha$ -pinene experiments, showing comparable magnitude in all three experiments (Full,  $\frac{1}{2}$  and  $\frac{1}{3}$  reactivity). By contrast, the average  $\overline{OSc}$  was influenced by the initial concentration of precursor in the single  $\alpha$ -pinene experiment obtained from the HR-ToF-AMS. The full reactivity of  $\alpha$ -pinene has lower  $\overline{OSc}$  (not accounting for  $\overline{OS_N}$ ) during SOA evolution than  $\frac{1}{2}$  reactivity  $\alpha$ -pinene, but higher than  $\frac{1}{3}$  reactivity experiment. The underlying causes of these differences are not yet well understood and require further investigation.

The average  $\overline{OSc}$  (not accounting for  $\overline{OS_N}$ ) in single precursor *o*-cresol experiment was not dependent on the initial concentration of precursor. CHON compounds have a significant influence on average  $\overline{OSc}$  of SOA in both the single VOC  $\alpha$ -pinene and *o*-cresol experiments, since the average  $\overline{OSc}$  (accounting for  $\overline{OS_N}$ ) has lower value than  $\overline{OSc}$  (not accounting for  $\overline{OS_N}$ ).

The isoprene experiments generating insignificant SOA particle mass (with total concentration in the full reactivity experiment never exceeding  $1 \mu\text{g m}^{-3}$ ) and so the trends in oxidation state were inaccessible. Isoprene only has a minor influence on the average carbon oxidation state of the SOA particles in the *o*-cresol/isoprene binary mixture, both trend and magnitude being almost identical to those in the single precursor *o*-cresol system. In contrast, the oxidation state decreased on addition of isoprene to  $\alpha$ -pinene, with the average in the  $\alpha$ -pinene/isoprene lower than the  $\alpha$ -pinene value. This may result from isoprene scavenging OH leading to suppression of low volatility  $\alpha$ -pinene driven oxygenated product formation. The degree of oxidation in the  $\alpha$ -pinene / *o*-cresol system was complex since both precursors generated considerable SOA mass, and  $\overline{OSc}$  was affected by both precursors, with products from both  $\alpha$ -pinene and *o*-cresol impacting on the oxidation state in the mixture. The  $\overline{OSc}$  shared similar trend with the sole  $\alpha$ -pinene experiment, with an increase in absolute value towards that of *o*-cresol. Compounds uniquely found in the mixture contributed to this behaviour. In the ternary precursor system, no single precursor dominated the oxidation state, though the general pattern was similar to that in the  $\alpha$ -pinene / *o*-cresol mixture. However, the addition of isoprene into ternary system leading to lower average carbon oxidation state compared to the  $\alpha$ -pinene / *o*-cresol binary system in the early stage of experiment, which may result from isoprene acting as OH scavenger in the same way as the  $\alpha$ -pinene/isoprene binary system.



~~This current study makes important first steps in the investigation of oxidation state in mixtures of SOA precursors, but reconciliation of the behaviour as revealed from different measurement techniques requires further work.~~

#### 1490 **Data availability**

All the data used in this work can be accessed on the open database of the EUROCHAMP programme (<https://data.eurochamp.org/data-access/chamber-experiments/>).

#### **Competing interests**

The authors declare that they have no conflict of interest.

#### 1495 **Author contributions**

GM, MRA, AV, YW and YS conceived the study. AV, YW, YS and MD conducted the experiments. TJB provided technical assistance during the experiments and contributed to the FIGAERO-CIMS data analysis. YS conducted the data analysis and wrote the manuscript with contribution from all co-authors.

1500

#### **Acknowledgements**

The Manchester Aerosol Chamber acknowledges the funding support from the European Union's Horizon 2020 research and innovation programme under grant agreement no. 730997, which supports the EUROCHAMP2020 research programme. Instrumentational support was funded by the NERC Atmospheric Measurement and Observational Facility (AMOF). Y.W. acknowledges the joint scholarship of The University of Manchester and Chinese Scholarship Council. M.R.A. acknowledges funding support by UK National Centre for Atmospheric Sciences (NACS). A.V. acknowledges the funding support by Natural Environment Research Council (NERC) EAO Doctoral Training Partnership. The authors would also like to thank Kelly Pereira for on-site UHPLC-HRMS training for filter analysis and for providing the automated non-targeted analysis method for UHPLC-HRMS. I acknowledge the use of ChatGPT AI tool to proof-reading and correct grammar at the final stage of the writing process for this paper, which I reviewed, edited, and take full responsibility for. All final wording reflects my own edits and judgment.

1515 **Reference**

- Ahlberg, E., Falk, J., Eriksson, A., Holst, T., Brune, W. H., Kristensson, A., Roldin, P., and Svenningsson, B.: Secondary organic aerosol from VOC mixtures in an oxidation flow reactor, *Atmospheric Environment*, 161, 210-220, <https://doi.org/10.1016/j.atmosenv.2017.05.005>, 2017.
- 1520 Aiken, A. C., DeCarlo, P. F., Kroll, J. H., Worsnop, D. R., Huffman, J. A., Docherty, K. S., Ulbrich, I. M., Mohr, C., Kimmel, J. R., Sueper, D., Sun, Y., Zhang, Q., Trimborn, A., Northway, M., Ziemann, P. J., Canagaratna, M. R., Onasch, T. B., Alfarra, M. R., Prevot, A. S. H., Dommen, J., Duplissy, J., Metzger, A., Baltensperger, U., and Jimenez, J. L.: O/C and OM/OC Ratios of Primary, Secondary, and Ambient Organic Aerosols with High-Resolution Time-of-Flight Aerosol Mass Spectrometry, *Environmental Science & Technology*, 42, 4478-4485, 10.1021/es703009q, 2008.
- 1525 Alfarra, M. R., Coe, H., Allan, J. D., Bower, K. N., Boudries, H., Canagaratna, M. R., Jimenez, J. L., Jayne, J. T., Garforth, A. A., Li, S.-M., and Worsnop, D. R.: Characterization of urban and rural organic particulate in the Lower Fraser Valley using two Aerodyne Aerosol Mass Spectrometers, *Atmospheric Environment*, 38, 5745-5758, <https://doi.org/10.1016/j.atmosenv.2004.01.054>, 2004.
- 1530 Atkinson, R. B., D. L. Cox, R. A. Crowley, J. N. Hampson, R. F. Hynes, R. G. Jenkin, M. E. Rossi, M. J. Troe, J.: Evaluated kinetic and photochemical data for atmospheric chemistry: Volume I - gas phase reactions of Ox, HOx, NOx and SOx species, *Atmos. Chem. Phys.*, 4, 1738, 10.5194/acp-4-1461-2004, 2004.
- 1535 Bruns, E. A., Perraud, V., Zelenyuk, A., Ezell, M. J., Johnson, S. N., Yu, Y., Imre, D., Finlayson-Pitts, B. J., and Alexander, M. L.: Comparison of FTIR and Particle Mass Spectrometry for the Measurement of Particulate Organic Nitrates, *Environmental Science & Technology*, 44, 1056-1061, 10.1021/es9029864, 2010.
- 1540 Carlton, A. G., Wiedinmyer, C., and Kroll, J. H.: A review of Secondary Organic Aerosol (SOA) formation from isoprene, *Atmos. Chem. Phys.*, 9, 4987-5005, 10.5194/acp-9-4987-2009, 2009.
- Chen, X., Li, K., Li, R., Fang, L., Bian, H., Jiang, W., Yan, C., and Du, L.: NOx-driven chemical transformation of terpene mixtures: Linking highly oxygenated organic molecules to health effects in secondary organic aerosol, *Journal of Environmental Sciences*, <https://doi.org/10.1016/j.jes.2025.09.004>, 2025.
- 1545 Chhabra, P. S., Flagan, R. C., and Seinfeld, J. H.: Elemental analysis of chamber organic aerosol using an aerodyne high-resolution aerosol mass spectrometer, *Atmos. Chem. Phys.*, 10, 4111-4131, 10.5194/acp-10-4111-2010, 2010.
- Cui, Y., Chen, K., Zhang, H., Lin, Y.-H., and Bahreini, R.: Chemical Composition and Optical Properties of Secondary Organic Aerosol from Photooxidation of Volatile Organic Compound Mixtures, *ACS ES&T Air*, 1, 247-258, 10.1021/acsestair.3c00041, 2024.
- 1550 D. Sueper and collaborators, 2020. ToF-AMS Data Analysis Software Webpage, [http://cires1.colorado.edu/jimenez-group/wiki/index.php/ToF-AMS\\_Analysis\\_Software](http://cires1.colorado.edu/jimenez-group/wiki/index.php/ToF-AMS_Analysis_Software)
- 1555 D'Ambro, E. L., Schobesberger, S., Gaston, C. J., Lopez-Hilfiker, F. D., Lee, B. H., Liu, J., Zelenyuk, A., Bell, D., Cappa, C. D., Helgestad, T., Li, Z., Guenther, A., Wang, J., Wise, M., Caylor, R., Surratt, J. D., Riedel, T., Hyttinen, N., Salo, V. T., Hasan, G., Kurtén, T., Shilling, J. E., and Thornton, J. A.: Chamber-based insights into the factors controlling epoxydiol (IEPOX)

- secondary organic aerosol (SOA) yield, composition, and volatility, *Atmos. Chem. Phys.*, 19, 11253-11265, 10.5194/acp-19-11253-2019, 2019.
- 1560 D'Ambro, E. L., Schobesberger, S., Gaston, C. J., Lopez-Hilfiker, F. D., Lee, B. H., Liu, J., Zelenyuk, A., Bell, D., Cappa, C. D., Helgestad, T., Li, Z., Guenther, A., Wang, J., Wise, M., Caylor, R., Surratt, J. D., Riedel, T., Hyttinen, N., Salo, V. T., Hasan, G., Kurtén, T., Shilling, J. E., and Thornton, J. A.: Chamber-based insights into the factors controlling epoxydiol (IEPOX) secondary organic aerosol (SOA) yield, composition, and volatility, *Atmos. Chem. Phys.*, 19, 11253-11265, 10.5194/acp-19-11253-2019, 2019.
- 1565 Daumit, K. E., Kessler, S. H., and Kroll, J. H.: Average chemical properties and potential formation pathways of highly oxidized organic aerosol, *Faraday Discuss*, 165, 181-202, 10.1039/c3fd00045a, 2013.
- DeCarlo, P. F., Kimmel, J. R., Trimborn, A., Northway, M. J., Jayne, J. T., Aiken, A. C., Gonin, M., Fuhrer, K., Horvath, T., Docherty, K. S., Worsnop, D. R., and Jimenez, J. L.: Field-Deployable, High-Resolution, Time-of-Flight Aerosol Mass Spectrometer, *Analytical Chemistry*, 78, 8281-8289, 10.1021/ac061249n, 2006.
- 1570 Dillon, T. J., Dulitz, K., Groß, C. B. M., and Crowley, J. N.: Temperature-dependent rate coefficients for the reactions of the hydroxyl radical with the atmospheric biogenics isoprene, alpha-pinene and delta-3-carene, *Atmos. Chem. Phys.*, 17, 15137-15150, 10.5194/acp-17-15137-2017, 2017.
- 1575 Docherty, K. S., Corse, E. W., Jaoui, M., Offenberg, J. H., Kleindienst, T. E., Krug, J. D., Riedel, T. P., and Lewandowski, M.: Trends in the oxidation and relative volatility of chamber-generated secondary organic aerosol, *Aerosol Science and Technology*, 52, 992-1004, 10.1080/02786826.2018.1500014, 2018.
- 1580 Du, M., Voliotis, A., Shao, Y., Wang, Y., Bannan, T. J., Pereira, K. L., Hamilton, J. F., Percival, C. J., Alfarra, M. R., and McFiggans, G.: Combined application of Online FIGAERO-CIMS and Offline LC-Orbitrap MS to Characterize the Chemical Composition of SOA in Smog Chamber Studies, *Atmos. Meas. Tech. Discuss.*, 2021, 1-42, 10.5194/amt-2021-420, 2021.
- 1585 Eddingsaas, N. C., Loza, C. L., Yee, L. D., Chan, M., Schilling, K. A., Chhabra, P. S., Seinfeld, J. H., and Wennberg, P. O.:  $\alpha$ -pinene photooxidation under controlled chemical conditions &ndash; Part 2: SOA yield and composition in low- and high-NO<sub>x</sub> environments, *Atmos. Chem. Phys.*, 12, 7413-7427, 10.5194/acp-12-7413-2012, 2012.
- Fry, J. L., Kiendler-Scharr, A., Rollins, A. W., Wooldridge, P. J., Brown, S. S., Fuchs, H., Dubé, W., Mensah, A., dal Maso, M., Tillmann, R., Dorn, H. P., Brauers, T., and Cohen, R. C.: Organic nitrate and secondary organic aerosol yield from NO<sub>3</sub> oxidation of  $\beta$ -pinene evaluated using a gas-phase kinetics/aerosol partitioning model, *Atmos. Chem. Phys.*, 9, 1431-1449, 10.5194/acp-9-1431-2009, 2009.
- 1590 Han, S., Li, Z., Lau, Y. S., Xiao, Y., Miljevic, B., Horchler, J., Li, J., Hu, W.-P., Wang, H., Wang, B., and Ristovski, Z.: Unraveling secondary organic aerosol formation from isoprene and toluene mixture, *npj Climate and Atmospheric Science*, 8, 311, 10.1038/s41612-025-01189-4, 2025.
- 1595 Hildebrandt, L., Henry, K. M., Kroll, J. H., Worsnop, D. R., Pandis, S. N., and Donahue, N. M.: Evaluating the Mixing of Organic Aerosol Components Using High-Resolution Aerosol Mass Spectrometry, *Environmental Science & Technology*, 45, 6329-6335, 10.1021/es200825g, 2011.
- 1600 Hoffmann, T., Huang, R.-J., and Kalberer, M.: *Atmospheric Analytical Chemistry*, *Analytical Chemistry*, 83, 4649-4664, 10.1021/ac2010718, 2011.

- Hoffmann, T., Odum, J. R., Bowman, F., Collins, D., Klockow, D., Flagan, R. C., and Seinfeld, J. H.: Formation of Organic Aerosols from the Oxidation of Biogenic Hydrocarbons, *Journal of Atmospheric Chemistry*, 26, 189-222, 10.1023/A:1005734301837, 1997.
- 1605 Jayne, J. T., Leard, D. C., Zhang, X., Davidovits, P., Smith, K. A., Kolb, C. E., and Worsnop, D. R.: Development of an aerosol mass spectrometer for size and composition analysis of submicron particles, *Aerosol Science & Technology*, 33, 49-70, 2000.
- Jimenez, J. L., Jayne, J. T., Shi, Q., Kolb, C. E., Worsnop, D. R., Yourshaw, I., Seinfeld, J. H., Flagan, R. C., Zhang, X., Smith, K. A., Morris, J. W., and Davidovits, P.: Ambient aerosol sampling using the Aerodyne Aerosol Mass Spectrometer, *Journal of Geophysical Research: Atmospheres*, 108, <https://doi.org/10.1029/2001JD001213>, 2003.
- 1610 Kroll, J. H., Lim, C. Y., Kessler, S. H., and Wilson, K. R.: Heterogeneous Oxidation of Atmospheric Organic Aerosol: Kinetics of Changes to the Amount and Oxidation State of Particle-Phase Organic Carbon, *The Journal of Physical Chemistry A*, 119, 10767-10783, 10.1021/acs.jpca.5b06946, 2015.
- 1615 Kroll, J. H., Ng, N. L., Murphy, S. M., Flagan, R. C., and Seinfeld, J. H.: Secondary organic aerosol formation from isoprene photooxidation under high-NO<sub>x</sub> conditions, *Geophysical Research Letters*, 32, <https://doi.org/10.1029/2005GL023637>, 2005a.
- Kroll, J. H., Ng, N. L., Murphy, S. M., Varutbangkul, V., Flagan, R. C., and Seinfeld, J. H.: Chamber studies of secondary organic aerosol growth by reactive uptake of simple carbonyl compounds, *Journal of Geophysical Research: Atmospheres*, 110, <https://doi.org/10.1029/2005JD006004>, 2005b.
- 1620 Kroll, J. H., Donahue, N. M., Jimenez, J. L., Kessler, S. H., Canagaratna, M. R., Wilson, K. R., Altieri, K. E., Mazzoleni, L. R., Wozniak, A. S., Bluhm, H., Mysak, E. R., Smith, J. D., Kolb, C. E., and Worsnop, D. R.: Carbon oxidation state as a metric for describing the chemistry of atmospheric organic aerosol, *Nature Chemistry*, 3, 133-139, 10.1038/nchem.948, 2011.
- 1625 Lee, B.-H., Pierce, J. R., Engelhart, G. J., and Pandis, S. N.: Volatility of secondary organic aerosol from the ozonolysis of monoterpenes, *Atmospheric Environment*, 45, 2443-2452, <https://doi.org/10.1016/j.atmosenv.2011.02.004>, 2011.
- 1630 Lee, B. H., Lopez-Hilfiker, F. D., Mohr, C., Kurtén, T., Worsnop, D. R., and Thornton, J. A.: An Iodide-Adduct High-Resolution Time-of-Flight Chemical-Ionization Mass Spectrometer: Application to Atmospheric Inorganic and Organic Compounds, *Environmental Science & Technology*, 48, 6309-6317, 10.1021/es500362a, 2014.
- Li, K., Zhang, X., Zhao, B., Bloss, W. J., Lin, C., White, S., Yu, H., Chen, L., Geng, C., Yang, W., Azzi, M., George, C., and Bai, Z.: Suppression of anthropogenic secondary organic aerosol formation by isoprene, *npj Climate and Atmospheric Science*, 5, 12, 10.1038/s41612-022-00233-x, 2022.
- 1635 Lopez-Hilfiker, F. D., Mohr, C., Ehn, M., Rubach, F., Kleist, E., Wildt, J., Mentel, T. F., Lutz, A., Hallquist, M., Worsnop, D., and Thornton, J. A.: A novel method for online analysis of gas and particle composition: description and evaluation of a Filter Inlet for Gases and AEROsols (FIGAERO), *Atmos. Meas. Tech.*, 7, 983-1001, 10.5194/amt-7-983-2014, 2014.
- 1640 McFiggans, G., Mentel, T. F., Wildt, J., Pullinen, I., Kang, S., Kleist, E., Schmitt, S., Springer, M., Tillmann, R., and Wu, C.: Secondary organic aerosol reduced by mixture of atmospheric vapours, *Nature*, 565, 587, 2019.

- 1645 Pandis, S. N., Paulson, S. E., Seinfeld, J. H., and Flagan, R. C.: Aerosol formation in the photooxidation of isoprene and  $\beta$ -pinene, *Atmospheric Environment. Part A. General Topics*, 25, 997-1008, [https://doi.org/10.1016/0960-1686\(91\)90141-S](https://doi.org/10.1016/0960-1686(91)90141-S), 1991.
- Pereira, K., Ward, M., Wilkinson, J., Sallach, J., Bryant, D., Dixon, W., Hamilton, J., and Lewis, A.: An Automated Methodology for Non-targeted Compositional Analysis of Small Molecules in High Complexity Environmental Matrices Using Coupled Ultra Performance Liquid
- 1650 Chromatography Orbitrap Mass Spectrometry, *Environmental Science & Technology*, XXXX, 10.1021/acs.est.0c08208, 2021.
- Presto, A. A., Miracolo, M. A., Kroll, J. H., Worsnop, D. R., Robinson, A. L., and Donahue, N. M.: Intermediate-Volatility Organic Compounds: A Potential Source of Ambient Oxidized Organic Aerosol, *Environmental Science & Technology*, 43, 4744-4749, 10.1021/es803219q, 2009.
- 1655 Pullinen, I., Schmitt, S., Kang, S., Sarrafzadeh, M., Schlag, P., Andres, S., Kleist, E., Mentel, T. F., Rohrer, F., Springer, M., Tillmann, R., Wildt, J., Wu, C., Zhao, D., Wahner, A., and Kiendler-Scharr, A.: Impact of NO<sub>x</sub> on secondary organic aerosol (SOA) formation from  $\alpha$ -pinene and  $\beta$ -pinene photooxidation: the role of highly oxygenated organic nitrates, *Atmos. Chem. Phys.*, 20, 10125-10147, 10.5194/acp-20-10125-2020, 2020.
- 1660 Shao, Y., Voliotis, A., Du, M., Wang, Y., Pereira, K., Hamilton, J., Alfarra, M. R., and McFiggans, G.: Chemical composition of secondary organic aerosol particles formed from mixtures of anthropogenic and biogenic precursors, *Atmos. Chem. Phys.*, 22, 9799-9826, 10.5194/acp-22-9799-2022, 2022a.
- Shao, Y., Wang, Y., Du, M., Voliotis, A., Alfarra, M. R., O'Meara, S. P., Turner, S. F., and
- 1665 McFiggans, G.: Characterisation of the Manchester Aerosol Chamber facility, *Atmos. Meas. Tech.*, 15, 539-559, 10.5194/amt-15-539-2022, 2022b.
- Shilling, J. E., Chen, Q., King, S. M., Rosenoern, T., Kroll, J. H., Worsnop, D. R., DeCarlo, P. F., Aiken, A. C., Sueper, D., Jimenez, J. L., and Martin, S. T.: Loading-dependent elemental composition of  $\alpha$ -pinene SOA particles, *Atmos. Chem. Phys.*, 9, 771-782, 10.5194/acp-9-771-
- 1670 2009, 2009.
- Stark, H., Yatavelli, R. L. N., Thompson, S. L., Kimmel, J. R., Cubison, M. J., Chhabra, P. S., Canagaratna, M. R., Jayne, J. T., Worsnop, D. R., and Jimenez, J. L.: Methods to extract molecular and bulk chemical information from series of complex mass spectra with limited mass resolution, *International Journal of Mass Spectrometry*, 389, 26-38,
- 1675 <https://doi.org/10.1016/j.ijms.2015.08.011>, 2015.
- Stroud, C. A., Roberts, J. M., Goldan, P. D., Kuster, W. C., Murphy, P. C., Williams, E. J., Hereid, D., Parrish, D., Sueper, D., Trainer, M., Fehsenfeld, F. C., Apel, E. C., Riemer, D., Wert, B., Henry, B., Fried, A., Martinez-Harder, M., Harder, H., Brune, W. H., Li, G., Xie, H., and Young, V. L.: Isoprene and its oxidation products, methacrolein and methylvinyl ketone, at an urban forested
- 1680 site during the 1999 Southern Oxidants Study, *Journal of Geophysical Research: Atmospheres*, 106, 8035-8046, <https://doi.org/10.1029/2000JD900628>, 2001.
- Surratt, J. D., Kroll, J. H., Kleindienst, T. E., Edney, E. O., Claeys, M., Sorooshian, A., Ng, N. L., Offenberg, J. H., Lewandowski, M., Jaoui, M., Flagan, R. C., and Seinfeld, J. H.: Evidence for Organosulfates in Secondary Organic Aerosol, *Environmental Science & Technology*, 41, 517-
- 1685 527, 10.1021/es062081q, 2007.
- Surratt, J. D., Gómez-González, Y., Chan, A. W. H., Vermeylen, R., Shahgholi, M., Kleindienst, T. E., Edney, E. O., Offenberg, J. H., Lewandowski, M., Jaoui, M., Maenhaut, W., Claeys, M., Flagan,

- R. C., and Seinfeld, J. H.: Organosulfate Formation in Biogenic Secondary Organic Aerosol, *The Journal of Physical Chemistry A*, 112, 8345-8378, 10.1021/jp802310p, 2008.
- 1690 Voliotis, A., Wang, Y., Shao, Y., Du, M., Bannan, T. J., Percival, C. J., Pandis, S. N., Alfarra, M. R., and McFiggans, G.: Exploring the composition and volatility of secondary organic aerosols in mixed anthropogenic and biogenic precursor systems, *Atmos. Chem. Phys. Discuss.*, 2021, 1-39, 10.5194/acp-2021-215, 2021.
- 1695 Voliotis, A., Du, M., Wang, Y., Shao, Y., Bannan, T. J., Flynn, M., Pandis, S. N., Percival, C. J., Alfarra, M. R., and McFiggans, G.: The influence of the addition of isoprene on the volatility of particles formed from the photo-oxidation of anthropogenic–biogenic mixtures, *Atmos. Chem. Phys.*, 22, 13677-13693, 10.5194/acp-22-13677-2022, 2022a.
- 1700 Voliotis, A., Du, M., Wang, Y., Shao, Y., Alfarra, M. R., Bannan, T. J., Hu, D., Pereira, K. L., Hamilton, J. F., Hallquist, M., Mentel, T. F., and McFiggans, G.: Chamber investigation of the formation and transformation of secondary organic aerosol in mixtures of biogenic and anthropogenic volatile organic compounds, *Atmos. Chem. Phys. Discuss.*, 2022, 1-49, 10.5194/acp-2021-1080, 2022b.
- 1705 Wennberg, P. O., Bates, K. H., Crounse, J. D., Dodson, L. G., McVay, R. C., Mertens, L. A., Nguyen, T. B., Praske, E., Schwantes, R. H., Smarte, M. D., St Clair, J. M., Teng, A. P., Zhang, X., and Seinfeld, J. H.: Gas-Phase Reactions of Isoprene and Its Major Oxidation Products, *Chemical Reviews*, 118, 3337-3390, 10.1021/acs.chemrev.7b00439, 2018.
- Winterhalter, R., Van Dingenen, R., Larsen, B. R., Jensen, N. R., and Hjorth, J.: LC-MS analysis of aerosol particles from the oxidation of  $\alpha$ -pinene by ozone and OH-radicals, *Atmos. Chem. Phys. Discuss.*, 2003, 1-39, 10.5194/acpd-3-1-2003, 2003.
- 1710 Xu, L., Middlebrook, A. M., Liao, J., de Gouw, J. A., Guo, H., Weber, R. J., Nenes, A., Lopez-Hilfiker, F. D., Lee, B. H., Thornton, J. A., Brock, C. A., Neuman, J. A., Nowak, J. B., Pollack, I. B., Welti, A., Graus, M., Warneke, C., and Ng, N. L.: Enhanced formation of isoprene-derived organic aerosol in sulfur-rich power plant plumes during Southeast Nexus, *Journal of Geophysical Research: Atmospheres*, 121, 11,137-111,153, 10.1002/2016jd025156, 2016.
- 1715 Zhao, Y., Zhao, Y., Wang, C., Shao, Y., Xie, H., Yang, J., Zhang, W., Wu, G., Li, G., Jiang, L., and Yang, X.: Photooxidation and ozonolysis of  $\alpha$ -pinene and limonene mixtures: Mechanisms of secondary organic aerosol formation and cross-dimerization, *Journal of Environmental Sciences*, <https://doi.org/10.1016/j.jes.2025.04.020>, 2025.

1720